The Star Formation Newsletter

A community newsletter on Star and Planet Formation research

No. 359 — 30 November 2022
Editor: João Alves www.starformation.news

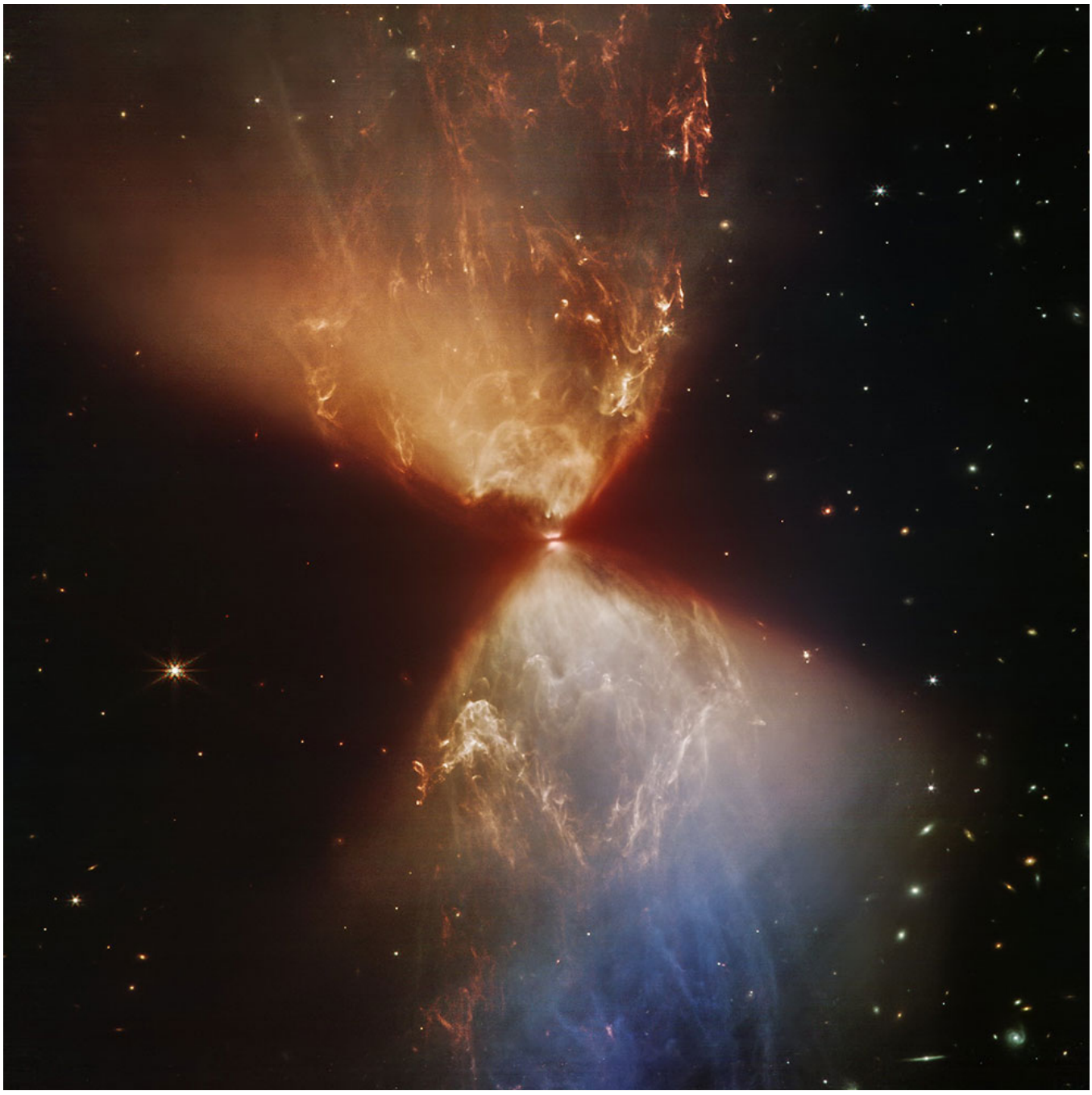

Links to sections

Interviews	Reviews	Perspective	Favorite objects	Archive
Meetings	Jobs	New PhDs	Announcements	Books

Cover image caption

JWST image of L1527 in the TMC ring, a classic revisited. L1527 is a Class 04 source, with an age of the order of 10^5 years. At a distance of about 140 pc to Earth, this object is one of the closest Class 0 objects to Earth. Credits: NASA, ESA, CSA, and STScI. Image processing: Judy Schmidt

Note from the Editor

The Star Formation Newsletter is now on the web at **www.starformation.news**. This PDF file contains the monthly Abstracts and links to the different Newsletter sections. Red text in this PDF is a url link. Submitting an abstract to the SFN is as simple as entering the arXiv ID (e.g., 2006.10139) in a web form on the SFN web site. **Do not remove the LaTeX formatting when submitting to the arXiv**. If you do, your abstract will not look great either at the arXiv or the SFN.

Abstracts

1. The Structure and 3D Kinematics of Vela OB2

Joseph J. Armstrong, Nicholas J. Wright, R. D. Jeffries, R. J. Jackson, T. Cantat-Gaudin ★ The kinematics of stars in OB associations can provide insights into their formation, dynamical evolution, and eventual fate. The low-mass stellar content of OB associations are sufficiently numerous as to provide a detailed sampling of their kinematic properties, however spectroscopy is required to confirm the youth of individual stars and to get 3D kinematics. In this paper we present and analyse results from a large spectroscopic survey of Vela OB2 conducted using 2dF/HERMES on the AAT. This spectroscopy is used to confirm the youth of candidate young stars and determine radial velocities, which are combined with proper motions and parallaxes from Gaia to measure 3-dimensional positions and velocities. We identify multiple separate kinematic groups in the region, for which we measure velocity dispersions and infer their virial states. We measure expansion rates for all these groups and find strong evidence for anisotropic expansion in the Vela OB2 association of at least 11σ significance in all three dimensions, as well as some evidence for expansion in the γ Vel and P Puppis clusters. We trace back the motions of these groups into the past and find that the open cluster NGC 2547 is an interloper in the Vela OB2 region and actually formed >100 pc away from the association. We conclude that Vela OB2 must have formed with considerable spatial and kinematic substructure over a timescale of ∼10 Myr, with clear temporal substructure within the association, but no clear evidence for an age gradient.

2. The Effect of Shock Wave Duration on Star Formation and the Initial Condition of Massive Cluster Formation

Daisei Abe, Tsuyoshi Inoue, Rei Enokiya, Yasuo Fukui ★ Stars are born in dense molecular filaments irrespective of their mass. Compression of the ISM by shocks cause filament formation in molecular clouds. Observations show that a massive star cluster formation occurs where the peak of gas column density in a cloud exceeds 10^{23} cm^{-2}. In this study, we investigate the effect of the shock-compressed layer duration on filament/star formation and how the initial conditions of massive star formation are realized by performing three-dimensional (3D) isothermal magnetohydrodynamics (MHD) simulations with gas inflow duration from the boundaries (i.e., shock wave duration) as a controlling parameter. Filaments formed behind the shock expand after the duration time for short shock duration models, whereas long duration models lead to star formation by forming massive supercritical filaments. Moreover, when the shock duration is longer than two postshock free-fall times, the peak column density of the compressed layer exceeds 10^{23} cm^{-2}, and the gravitational collapse of the layer causes that the number of OB stars expected to be formed in the shock-compressed layer reaches the order of ten (i.e., massive cluster formation).

3. The kinematics and excitation of infrared water vapor emission from planet-forming disks: results from spectrally-resolved surveys and guidelines for JWST spectra

Andrea Banzatti, Klaus M. Pontoppidan, José Pérez Chávez, Colette Salyk, Lindsey Diehl, Simon Bruderer, Greg J. Herczeg, Andres Carmona, Ilaria Pascucci, Sean Brittain, Stanley Jensen, Sierra Grant, Ewine F. van Dishoeck, Inga Kamp, Arthur D. Bosman, Karin I. Öberg, Geoff A. Blake, Michael R. Meyer, Eric Gaidos, Adwin Boogert, John T. Rayner, Caleb Wheeler ★ This work presents ground-based spectrally-resolved water emission at R = 30000-100000 over infrared wavelengths covered by JWST (2.9-12.8 μm). Two new surveys with iSHELL and VISIR are combined with previous spectra from CRIRES and TEXES to cover parts of multiple ro-vibrational and rotational bands observable within telluric transmission bands, for a total of $\approx$ 160 spectra and 85 disks (30 of which are JWST targets in Cycle 1). The general expectation of a range of regions and excitation conditions traced by infrared water spectra is for the first time supported by the combined kinematics and excitation as spectrally resolved at multiple wavelengths. The main findings from this analysis are: 1) water lines are progressively narrower from the ro-vibrational bands at 2-9 μm to the rotational lines at 12 μm, and partly match a broad (BC) and narrow (NC) emission components, respectively, as extracted from ro-vibrational CO spectra; 2) rotation diagrams of resolved water lines from upper level energies of 4000-9500 K show vertical spread and curvatures indicative of optically thick emission ($\approx 10^{18}$ cm^{-2}) from a range of excitation temperatures ($\approx$ 800-1100 K); 3) the new 5 μm spectra demonstrate that slab model fits to the rotational lines at $>$ 10 μm strongly over-predict the ro-vibrational emission bands at $<$ 9 μm, implying non-LTE vibrational excitation. We discuss these findings in the context of emission from a disk surface and a molecular inner disk wind, and provide a list of guidelines to support the analysis of spectrally-unresolved JWST spectra.

4. Rapid Formation of Exoplanetesimals Revealed by White Dwarfs

A. Bonsor, T. Lichtenberg, J. Drazkowska, A. M. Buchan ★ The timing of formation for the first planetesimals determines the mode of planetary accretion and their geophysical and compositional evolution. Astronomical observations of circumstellar discs and Solar System geochronology provide evidence for planetesimal formation during molecular cloud collapse, much earlier than previously estimated. Here, we present distinct observational evidence from white dwarf planetary systems for planetesimal formation occurring during the first few hundred thousand years after cloud collapse in exoplanetary systems. A significant fraction of white dwarfs have accreted planetary material rich in iron core or mantle material. In order for the exo-asteroids accreted by white dwarfs to form iron cores, substantial heating is required. By simulating planetesimal evolution and collisional evolution we show that the most likely heat source is short-lived radioactive nuclides such as Al-2 (half life of approximately 0.7 Myr). Core-rich materials in the atmospheres of white dwarfs, therefore, provide independent evidence for rapid planetesimal formation, concurrent with star formation.

5. *L*-band Spectra of Young Brown Dwarfs

Samuel Beiler, Katelyn Allers, Michael Cushing, Jacqueline Faherty, Mark Marley, Andrew Skemer ★ We present a L-band (2.98–3.96μm) spectroscopic study of 8 young L dwarfs with spectral types ranging from L2 to L7. Our spectra ($\lambda/\Delta\lambda \approx 250$ to 600) were collected using the Gemini Near-InfraRed Spectrograph. We first examine the young L-band spectral sequence, most notably analyzing the evolution of the Q-branch of methane absorption feature at 3.3 μm. We find the Q-branch feature first appears between L3 and L6, as previously seen in older field dwarfs. Secondly, we analyze how well various atmospheric models reproduce the L-band and published near-IR (0.7–2.5 μm) spectra of our objects by fitting five different grids of model spectra to the data. Best-fit parameters for the combined near-IR and L-band data are compared to best-fit parameters for just the near-IR data, isolating the impact that the addition of the L-band has on the results. This addition notably causes a $\sim$100 K drop in the best-fit effective temperature. Also, when clouds and a vertical mixing rate (K_{zz}) are included in the models, thick clouds and higher K_{zz} values are preferred. Five of our objects also have previously published effective temperatures and surface gravities derived using evolutionary models, age estimates, and bolometric luminosities. Comparing model spectra matching these parameters to our spectra, we find disequilibrium chemistry and clouds are needed to match these published effective temperatures. Three of these objects are members of AB Dor, allowing us to show the temperature dependence of the Q-branch of methane.

6. PDFchem: A new fast method to determine ISM properties and infer environmental parameters using probability distributions

Thomas G. Bisbas, Ewine F. van Dishoeck, Chia-Yu Hu, Andreas Schruba ★ Determining the atomic and molecular content of the interstellar medium (ISM) as a function of environmental parameters is of fundamental importance to understand the star-formation process across the epochs. Although there exist various three-dimensional hydro-chemical codes modelling the ISM at different scales and redshifts, they are computationally expensive and inefficient for studies over a large parameter space. Building on our earlier approach, we present PDFchem, a novel algorithm that models the cold ISM at moderate and large scales using functions connecting the quantities of the local ($A_{V,eff}$) and the observed ($A_{V,obs}$) visual extinctions, and the local number density, n_H, with probability density functions (PDF) of $A_{V,obs}$ on cloud scales typically tens-to-hundreds of

pc as an input. For any given $A_{\rm V,obs}$-PDF, sampled with thousands of clouds, the algorithm instantly computes the average abundances of the most important species (HI, H_2, CII, CI, CO, OH, OH^+, H_2O^+, CH, HCO^+) and performs radiative transfer calculations to estimate the average emission of the most commonly observed lines ([CII] 158μm, both [CI] fine-structure lines and the first five rotational transitions of ^{12}CO). We examine two $A_{\rm V,obs}$-PDFs corresponding to a non star-forming and a star-forming ISM region, under a variety of environmental parameters combinations. These cover FUV intensities in the range of $\chi/\chi_0 = 10^{-1} - 10^3$, cosmic-ray ionization rates in the range of $\zeta_{\rm CR} = 10^{-17} - 10^{-13}\,{\rm s}^{-1}$ and metallicities in the range of $Z = 0.1 - 2\,{\rm Z}_\odot$. PDFchem is fast, easy to use, reproduces the PDR quantities of the time-consuming hydrodynamical models and can be used directly with observed data to understand the evolution of the cold ISM chemistry.

7. The statistical properties of stars at redshift, z=5, compared with the present epoch

Matthew R. Bate ★ We report the statistical properties of stars and brown dwarfs obtained from three radiation hydrodynamical simulations of star cluster formation with metallicities of 1, 1/10 and 1/100 of the solar value. The star-forming clouds are subjected to cosmic microwave background radiation that is appropriate for star formation at a redshift z=5. The results from the three calculations are compared to each other, and to similar previously published calculations that had levels of background radiation appropriate for present-day (z=0) star formation. Each of the calculations treat dust and gas temperatures separately and include a thermochemical model of the diffuse interstellar medium. We find that whereas the stellar mass distribution is insensitive to the metallicity for present-day star formation, at z=5 the characteristic stellar mass increases with increasing metallicity and the mass distribution has a deficit of brown dwarfs and low-mass stars at solar metallicity compared to the Galactic initial mass function. We also find that the multiplicity of M-dwarfs decreases with increasing metallicity at z=5. These effects are a result of metal-rich gas being unable to cool to as low temperatures at z=5 compared to at z=0 due to the hotter cosmic microwave background radiation, which inhibits fragmentation at high densities.

8. Measuring Optical Extinction Towards Young Stellar Objects Using Diffuse Interstellar Bands

Adolfo S. Carvalho, Lynne A. Hillenbrand ★ Line-of-sight extinction estimates to well-studied young T Tauri and Herbig Ae/Be stars are based on many different measurements and analysis methods. This has resulted in wide scatter among the published A_V values for the same star. In this work, we discuss the challenges in measuring extinction to actively accreting and especially outbursting young stellar objects (YSOs). We then explore a method not previously applied to young stars utilizing diffuse interstellar bands (DIBs). In early-type stars, narrow correlations exist between DIB equivalent widths and the column density of interstellar material, and therefore the line-of-sight extinction. Here, we measure equivalent widths of the 5780 Å and 6614 Å DIB features in a sample of actively accreting YSOs, and apply a DIB-reddening calibration to estimate reddening and subsequently extinction. Our calibration is newly derived from a composite of available literature data and fully accounts for the scatter in these measurements. We also compare the DIBs-inferred optical line-of-sight extinction values with previous extinction estimates for our sample stars.

9. The GRAVITY Young Stellar Object survey – IX. Spatially resolved kinematics of hot hydrogen gas in the star/disk interaction region of T Tauri stars

GRAVITY Collaboration, J. A. Wojtczak et al. ★ Aims: We aim to spatially and spectrally resolve the Br-gamma hydrogen emission line with the methods of interferometry in order to examine the kinematics of the hydrogen gas emission region in the inner accretion disk of a sample of solar-like young stellar objects. The goal is to identify trends and categories among the sources of our sample and to discuss whether or not they can be tied to different origin mechanisms associated with Br-gamma emission in T Tauri stars, chiefly and most prominently magnetospheric accretion. Methods: We observed a sample of seven T Tauri stars for the first time with VLTI GRAVITY, recording spectra and spectrally dispersed interferometric quantities across the Br-gamma line in the NIR K-band. We use them to extract the size of the Br-gamma emission region and the photocenter shifts. To assist in the interpretation, we also make use of radiative transfer models of magnetospheric accretion to establish a baseline of expected interferometric signatures if accretion is the primary driver of Br-gamma emission. Results: From among our sample, we find that five of the seven T Tauri stars show an emission region with a half-flux radius in the range broadly expected for magnetospheric truncation. Two of the five objects also show Br-gamma emission primarily originating from within the corotation radius, while two other objects exhibit extended emission on a scale beyond 10 R_*, one of them even beyond the K band continuum half-flux radius of 11.3 R_*. Conclusions: We find strong evidence to suggest that for the two weakest accretors in the sample, magnetospheric accretion is the primary driver of Br-gamma radiation. The results for the remaining sources imply either partial or strong contributions coming from spatially extended emission components in the form of outflows, such as stellar or disk winds.

10. Pre-main Sequence Brackett Emitters in the APOGEE DR17 Catalog: Line Strengths and Physical Properties of Accretion Columns

Hunter Campbell, Elliott Khilfeh, Kevin R. Covey, Marina Kounkel, Richard Ballantyne, Sabrina Corey, Carlos G. Román-Zúñiga, Jesús Hernández, Ezequiel Manzo Martínez, Karla Peña Ramírez, Alexandre Roman-Lopes, Keivan G. Stassun, Guy S. Stringfellow, Jura Borissova, S. Drew Chojnowski, Valeria Ramírez-Preciado, Jinyoung Serena Kim, Javier Serna, Amelia M. Stutz, Ricardo López-Valdivia, Genaro Suárez, Jason E. Ybarra, Penélope Longa-Peña, José G. Fernández-Trincado ★ Very young (t $\lesssim$ 10 Myrs) stars possess strong magnetic fields that channel ionized gas from the interiors of their circumstellar discs to the surface of the star. Upon impacting the stellar surface, the shocked gas recombines and emits hydrogen spectral lines. To characterize the density and temperature of the gas within these accretion streams, we measure equivalent widths of Brackett (Br) 11-20 emission lines detected in 1101 APOGEE spectra of 326 likely pre-main sequence accretors. For sources with multiple observations, we measure median epoch-to-epoch line strength variations of 10% in Br11 and 20% in Br20. We also fit the measured line ratios to predictions of radiative transfer models by Kwan & Fischer. We find characteristic best-fit electron densities of $n_e = 10^{11} - 10^{12}$ cm^{-3}, and excitation temperatures that are inversely correlated with electron density (from T$\sim$5000 K for $n_e \sim 10^{12}$ cm^{-3}, to T$\sim$12500 K at $n_e \sim 10^{11}$ cm^{-3}). These physical parameters are in good agreement with predictions from modelling of accretion streams that account for the hydrodynamics and radiative transfer within the accretion stream. We also present a supplementary catalog of line measurements from 9733 spectra of 4255 Brackett emission line sources in the APOGEE DR17 dataset.

11. Evaporation before disruption: comparing timescales for Jovian planets in star-forming regions

Emma C. Daffern-Powell, Richard J. Parker ★ Simulations show that the orbits of planets are readily disrupted in dense star-forming regions; planets can be exchanged between stars, become free-floating and then be captured by other stars. However, dense star-forming regions also tend to be populous, containing massive stars that emit photoionising radiation, which can evaporate the gas in protoplanetary discs. We analyse N-body simulations of star-forming regions containing Jovian-mass planets and determine the times when their orbits are altered, when they become free-floating, and when they are stolen or captured. Simultaneously, we perform calculations of the evolution of protoplanetary discs when exposed to FUV radiation fields from massive stars in the same star-forming regions. In almost half (44 per cent) of the planetary systems that are disrupted - either altered, captured, stolen or become free-floating, we find that the radius of the protoplanetary disc evolves inwards, or the gas in the disc is completely evaporated, before the planets' orbits are disrupted. This implies that planets that are disrupted in dense, populous star-forming regions are more likely to be super Earths or mini Neptunes, as Jovian mass planets would not be able to form due to mass loss from photoevaporation. Furthermore, the recent discoveries of distant Jovian mass planets around tightly-packed terrestrial planets argue against their formation in populous star-forming regions, as photoevaporation would preclude gas giant planet formation at distances of more than a few au.

12. The Star Formation Rate of the Milky Way as seen by Herschel

D. Elia, S. Molinari, E. Schisano, J. D. Soler, M. Merello, D. Russeil, M. Veneziani, A. Zavagno, A. Noriega-Crespo, L. Olmi, M. Benedettini, P. Hennebelle, R. S. Klessen, S. Leurini, R. Paladini, S. Pezzuto, A. Traficante, D. J. Eden, P. G. Martin, M. Sormani, A. Coletta, T. Colman, R. Plume, Y. Maruccia, C. Mininni, S. J. Liu ★ We present a new derivation of the Milky Way's current star formation rate (SFR) based on the data of the Hi-GAL Galactic plane survey. We estimate the distribution of the SFR across the Galactic plane from the star-forming clumps identified in the Hi-GAL survey and calculate the total SFR from the sum of their contributions. The estimate of the global SFR amounts to 2.0 ± 0.7 M$_\odot$ yr^{-1}, of which 1.7 ± 0.6 M$_\odot$ yr^{-1} coming from clumps with reliable heliocentric distance assignment. This value is in general agreement with estimates found in the literature of last decades. The profile of SFR density averaged in Galactocentric rings is found to be qualitatively similar to others previously computed, with a peak corresponding to the Central Molecular Zone and another one around Galactocentric radius $R_{\rm gal} \sim 5$ kpc, followed by an exponential decrease as $\log(\Sigma_{\rm SFR}/[\mathrm{M}_\odot\ \mathrm{yr}^{-1}\ \mathrm{kpc}^{-2}]) = a\, R_{\rm gal}/[\mathrm{kpc}] + b$, with $a = -0.28 \pm 0.01$. In this regard, the fraction of SFR produced within and outside the Solar circle is 84% and 16%, respectively; the fraction corresponding to the far outer Galaxy ($R_{\rm gal} > 13.5$ kpc) is only 1%. We also find that, for $R_{\rm gal} > 3$ kpc, our data follow a power law as a function of density, similarly to the Kennicutt-Schmidt relation. Finally, we compare the distribution of the SFR density across the face-on Galactic plane and those of median parameters, such as temperature, luminosity/mass ratio and bolometric temperature, describing the evolutionary stage of Hi-GAL clumps. We found no clear correlation between the SFR and the clump evolutionary stage.

13. Modelling photo-evaporation in planet forming discs

Barbara Ercolano, Giovanni Picogna ★ Planets are born from the gas and dust discs surrounding young stars. Energetic radiation from the central star can drive thermal outflows from the discs atmospheres, strongly affecting the evolution of the discs and the nascent planetary system. In this context several numerical models of varying complexity have been developed to study the process of disc photoevaporation from their central stars. We describe the numerical techniques, the results and the

predictivity of current models and identify observational tests to constrain them.

14. The Small Separation A-Star Companion Population: First Results with CHARA/MIRC-X

Matthew De Furio, Tyler Gardner, John Monnier, Michael R. Meyer, Kaitlin Kratter, Gail Schaefer, Narsireddy Anugu, Claire L. Davies, Stefan Kraus, Cyprien Lanthermann, Jean-Baptiste Le Bouquin, Jacob Ennis
★ We present preliminary results from our long-baseline interferometry (LBI) survey to constrain the multiplicity properties of intermediate-mass A-type stars within 80pc. Previous multiplicity studies of nearby stars exhibit orbital separation distributions well-fitted with a log-normal with peaks $>$ 15au, increasing with primary mass. The A-star multiplicity survey of De Rosa et al. (2014), sensitive beyond 30au but incomplete below 100 au, found a log-normal peak around 390au. Radial velocity surveys of slowly-rotating, chemically peculiar Am stars identified a significant number of very close companions with periods $\leq$ 5 days, 0.1au, a result similar to surveys of O- and B-type primaries. With the improved performance of LBI techniques, we can probe these close separations for normal A-type stars where other surveys are incomplete. Our initial sample consists of 27 A-type primaries with estimated masses between 1.44-2.49M$_\odot$ and ages 10-790Myr, which we observed with the MIRC-X instrument at the CHARA Array. We use the open source software CANDID to detect five companions, three of which are new, and derive a companion frequency of $0.19^{+0.11}_{-0.06}$ over mass ratios 0.25-1.0 and projected separations 0.288-5.481 au. We find a probability of 10^{-6} that our results are consistent with extrapolations based on previous models of the A-star companion population, over mass ratios and separations sampled. Our results show the need to explore these very close separations to inform our understanding of stellar formation and evolution processes.

15. Demographics of the M-star Multiple Population in the Orion Nebula Cluster

Matthew De Furio, Christopher Liu, Michael R. Meyer, Megan Reiter, Adam Kraus, Trent Dupuy, John Monnier
★ We present updated results constraining multiplicity demographics for the stellar population of the Orion Nebula Cluster (ONC, a high-mass, high-density star-forming region), across primary masses 0.08-0.7M$_\odot$. Our study utilizes archival Hubble Space Telescope data obtained with the Advanced Camera for Surveys using multiple filters (GO-10246). Previous multiplicity surveys in low-mass, low-density associations like Taurus identify an excess of companions to low-mass stars roughly twice that of the Galactic field and find the mass ratio distribution consistent with the field. Previously, we found the companion frequency to low-mass stars in the ONC is consistent with the Galactic field over mass ratios=0.6-1.0 and projected separations=30-160au, without placing constraints on the mass ratio distribution. In this study, we investigate the companion population of the ONC with a double point-spread function (PSF) fitting algorithm sensitive to separations larger than 10au (0.025") using empirical PSF models. We identified 44 companions (14 new), and with a Bayesian analysis, estimate the companion frequency to low-mass stars in the ONC $=0.13^{+0.05}_{-0.03}$ and the power law fit index to the mass ratio distribution $=2.08^{+1.03}_{-0.85}$ over all mass ratios and projected separations of 10-200au. We find the companion frequency in the ONC is consistent with the Galactic field population, likely from high transient stellar density states, and a probability of 0.002 that it is consistent with that of Taurus. We also find the ONC mass ratio distribution is consistent with the field and Taurus, potentially indicative of its primordial nature, a direct outcome of the star formation process.

16. The Giant Accreting Protoplanet Survey (GAPlanetS) – Results from a Six Year Campaign to Image Accreting Protoplanets

Katherine B. Follette, Laird M. Close, Jared R. Males, Kimberly Ward-Duong, William O. Balmer, Jea Adams Redai, Julio Morales, Catherine Sarosi, Beck Dacus, Robert J. De Rosa, Fernando Garcia Toro, Clare Leonard, Bruce Macintosh, Katie M. Morzinski, Wyatt Mullen, Joseph Palmo, Raymond Nzaba Saitoti, Elijah Spiro, Helena Treiber, Jason Wang, David Wang, Alex Watson, Alycia J. Weinberger
★ Accreting protoplanets represent a window into planet formation processes. We report H$_\alpha$ differential imaging results from the deepest and most comprehensive accreting protoplanet survey to date, acquired with the Magellan Adaptive Optics (MagAO) system's VisAO camera. The fourteen transitional disks targeted are ideal candidates for protoplanet discovery due to their wide, heavily depleted central cavities, wealth of non-axisymmetric circumstellar disk features evocative of ongoing planet formation, and ongoing stellar accretion. To address the twin challenges of morphological complexity in the target systems and PSF instability, we develop novel approaches for frame selection and optimization of the Karhounen-Loeve Image Processing algorithm pyKLIP. We detect one new candidate protoplanet, CS Cha "c", at a separation of 75mas and a Δmag of 5.1 and robustly recover the HD142527 B and HD100453 B low mass stellar companions across multiple epochs. Though we cannot rule out a substantial scattered light contribution to its emission, we also recover LkCa 15 b. Its presence inside of the cleared disk cavity and consistency with a forward-modeled point source suggest that it remains a viable protoplanet candidate. The protoplanet PDS 70 c was marginally recovered under our conservative general methodology. However, through targeted optimization in H$_\alpha$ imagery, we tentatively recover PDS 70 c in three epochs and PDS 70 b in one epoch. Of the many other previously-reported companions and companion candidates around objects in the sample, we do not recover any additional robust candidates. However, lack of

recovery at moderate H_α contrast does not rule out the presence of protoplanets at these locations, and we report limiting H_α contrasts in such cases.

17. The Mass Accretion Rate and Stellar Properties in Class I Protostars

Eleonora Fiorellino, Lukasz Tychoniec, Fernando Cruz-Saenz de Miera, Simone Antoniucci, Agnes Kospal, Carlo F. Manara, Brunella Nisini, Giovanni Rosotti ★ Stars collect most of their mass during the protostellar stage, yet the accretion luminosity and stellar parameters, which are needed to compute the mass accretion rate, are poorly constrained for the youngest sources. The aim of this work is to fill this gap, computing the stellar properties and the accretion rates for a large sample of Class I protostars located in nearby (< 500 pc) star-forming regions and analysing their interplay. We used a self-consistent method to provide accretion and stellar parameters using SED modeling and veiling information from near-IR observations, when possible. We calculated accretion and stellar properties for the first time for 50 young stars. We focused our analysis on the 39 confirmed protostars, finding that their mass accretion rate varies between about 10^{-8} and about 10^{-4} Msun/yr in a stellar mass range between about 0.1 and 3 Msun. We find systematically larger mass accretion rates for our Class I sample than in Class II objects. Although the mass accretion rate we found is high, it still suggests that either stars collect most of its mass before Class I stage, or eruptive accretion is needed during the overall protostellar phase. Indeed, our results suggest that for a large number of protostars the disk can be unstable, which can result in accretion bursts and disk fragmentation in the past or in the future.

18. Twisted magnetic field in star formation processes of L1521 F revealed by submillimeter dual band polarimetry using James Clerk Maxwell Telescope

Sakiko Fukaya, Hiroko Shinnaga, Ray S. Furuya, Kohji Tomisaka, Masahiro N. Machida, Naoto Harada ★ Understanding the initial conditions of star formation requires both observational studies and theoretical works taking into account the magnetic field, which plays an important role in star formation processes. Herein, we study the young nearby dense cloud core L1521 F ($n(H_2) \sim 10^{4-6}$ cm^{-3}) in the Taurus Molecular Cloud. This dense core hosts a 0.2 $M_\odot$ protostar, categorized as a Very Low Luminosity Objects with complex velocity structures, particularly in the vicinity of the protostar. To trace the magnetic field within the dense core, we conducted high sensitivity submillimeter polarimetry of the dust continuum at λ= 850 μm and 450 μm using the POL-2 polarimeter situated in front of the SCUBA-2 submillimeter bolometer camera on James Clerk Maxwell Tetescope. This was compared with millimeter polarimetry taken at λ= 3.3 mm with ALMA. The magnetic field was detected at λ= 850 μm in the peripheral region, which is threaded in a north-south direction, while the central region traced at λ= 450 μm shows a magnetic field with an east-west direction, i.e., orthogonal to that of the peripheral region. Magnetic field strengths are estimated to be ∼70 μG and 200 μG in the peripheral- and central-regions, respectively, using the Davis-Chandrasekhar-Fermi method. The resulting mass-to-flux ratio of 3 times larger than that of magnetically critical state for both regions indicates that L1521 F is magnetically supercritical, i.e., gravitational forces dominate over magnetic turbulence forces. Combining observational data with MHD simulations, detailed parameters of the morphological properties of this puzzling object are derived for the first time.

19. Spatial and dynamical structure of the NGC 2264 star-forming region

E. Flaccomio, G. Micela, G. Peres, S. Sciortino, E. Salvaggio, L. Prisinzano, M. G. Guarcello, L. Venuti, R. Bonito, I. Pillitteri ★ The processes that lead from molecular clouds to protostars, stellar associations, and the evolution of both, are active research topics. The target of this study, NGC2264, is a benchmark star-forming region (SFR) in which these issues can be profitably studied. We assembled a new extensive sample of NGC 2264 members. To this end we used new X-ray data obtained with the XMM-Newton telescope, GAIA eDR3 data, and an extensive collection of public and published catalogs. Following a previous suggestion that the SFR might extend significantly beyond the better studied areas, our search covers a wide 2.5x2.5 degrees region in the sky. Our catalog comprises more than 2200 candidate members, a 100% increase over previous determinations. We analyze their spatial distribution and define new substructures. Using GAIA parallaxes we estimate a new average distance to NGC2264 of 722+/-2pc and suggest that the embedded Spokes subregion is 20pc farther away within the molecular cloud. A complex dynamics is unveiled by the available proper motions and radial velocities: we observe signs of global expansion and rotation. At the same time, we observe the collapse and coalescence of two substructures in a region where active star formation is taking place. The fraction of stars with disks and of those undergoing circumstellar accretion varies significantly across the field, suggesting that star formation has been occurring for several million years. A particularly low disk fraction around the O VII star S Mon might be attributed to external disk photoevaporation or to an older age of the stars in the region. NGC2264 is not dynamically relaxed and its present configuration is the result of multiple dynamical processes. The cloud has been forming stars for several million years and we identify the process that is likely responsible for the ongoing formation activity.

20. The SPHERE view of multiple star formation

R. Gratton, S. Desidera, F. Marzari, M. Bonavita ★ While a large fraction of the stars are in multiple systems, our understanding of the processes leading to the formation of these systems is still inadequate. Given the large theoretical uncertainties, observation plays a basic role. Here we discuss the contribution of high contrast imaging, and more specifically of the SPHERE instrument at the ESO Very Large Telescope, in this area. SPHERE nicely complements other techniques - in particular those exploiting Gaia and ALMA - in detecting and characterising systems near the peak of the distribution with separation and allows to capture snapshots of binary formation within disks that are invaluable for the understanding of disk fragmentation.

21. Salt-bearing disk candidates around high-mass young stellar objects

Adam Ginsburg, Brett A. McGuire, Patricio Sanhueza, Fernando Olguin, Luke T Maud, Kei E. I. Tanaka, Yichen Zhang, Henrik Beuther, Nick Indriolo ★ Molecular lines tracing the orbital motion of gas in a well-defined disk are valuable tools for inferring both the properties of the disk and the star it surrounds. Lines that arise only from a disk, and not also from the surrounding molecular cloud core that birthed the star or from the outflow it drives, are rare. Several such emission lines have recently been discovered in one example case, those from NaCl and KCl salt molecules. We studied a sample of 23 candidate high-mass young stellar objects (HMYSOs) in 17 high-mass star-forming regions to determine how frequently emission from these species is detected. We present five new detections of water, NaCl, KCl, PN, and SiS from the innermost regions around the objects, bringing the total number of known briny disk candidates to nine. Their kinematic structure is generally disk-like, though we are unable to determine whether they arise from a disk or outflow in the sources with new detections. We demonstrate that these species are spatially coincident in a few resolved cases and show that they are generally detected together, suggesting a common origin or excitation mechanism. We also show that several disks around HMYSOs clearly do not exhibit emission in these species. Salty disks are therefore neither particularly rare in high-mass disks, nor are they ubiquitous.

22. Ammonia, carbon dioxide and the non-detection of the 2152 cm^{-1} CO band

Jiao He, Giulia Perotti, Shahnewaz M. Emtiaz, Francis E. Toriello, Adwin Boogert, Thomas Henning, Gianfranco Vidali ★ CO is one of the most abundant ice components on interstellar dust grains. When it is mixed with amorphous solid water (ASW) or located on its surface, an absorption band of CO at 2152 cm^{-1} is always present in laboratory measurements. This spectral feature is attributed to the interaction of CO with dangling-OH bonds (dOH) in ASW. However, this band is absent in observational spectra of interstellar ices. This raises the question whether CO forms a relatively pure layer on top of ASW or is in close contact with ASW, but not via dangling bonds. We aim to determine whether the incorporation of NH_3 or CO_2 into ASW blocks the dOH and therefore reduces the 2152 cm^{-1} band. We performed laboratory experiments to simulate the layered structure of the ice mantle, that is, we grew CO ice on top of 1) pure ASW, 2) NH_3:H_2O=10:100 mixed ice, and 3) CO_2:H_2O=20:100 mixed ice. Infrared spectra were measured to quantify the strength of the 2152 cm^{-1} band. In addition, a second set of experiments were performed to determine how the incorporation of NH_3 into ASW affects the dOH band. We found that annealing the ice reduces the 2152 cm^{-1} band and that NH_3 blocks the dOH on ASW surface and therefore reduces the 2152 cm^{-1} band more effectively than CO_2. We suggest that this difference between NH_3 and CO_2 can be ascribed to the polarity of the guest molecule (NH_3 is a polar species, whereas CO_2 is apolar). The polarity implies that the formation of an H-bond between the N atom of ammonia and the dOH is a barrier-less reaction. We also determined the pore surface area of the ice mixtures as a function of the annealing temperature, and found that the nondetection of 2152 cm^{-1} band does not necessarily exclude the possibility of a porous ice mantle.

23. Grain Growth in the Dust Ring with Crescent around Very Low Mass Star ZZ Tau IRS with JVLA

Jun Hashimoto, Hauyu Baobab Liu, Ruobing Dong, Beibei Liu, Takayuki Muto ★ The azimuthal asymmetries of dust rings in protoplanetary disks such as a crescent around young stars are often interpreted as dust traps, and thus as ideal locations for planetesimal and planet formations. Whether such dust traps effectively promote planetesimal formation in disks around very-low-mass stars (VLM; a mass of $\lesssim$0.2 $M_\odot$) is debatable, as the dynamical and grain growth timescales in such systems are long. To investigate grain growth in such systems, we studied the dust ring with crescent around the VLM star ZZ Tau IRS using the Karl G. Jansky Very Large Array (JVLA) at centimeter wavelengths. Significant signals were detected around ZZ Tau IRS. To estimate the maximum grain size ($a_{\rm max}$) in the crescent, we compared the observed spectral energy distribution (SED) with SEDs for various $a_{\rm max}$ values predicted by radiative transfer calculations. We found $a_{\rm max} \gtrsim 1$ mm and $\lesssim 60$ μm in the crescent and ring, respectively, though our modeling efforts rely on uncertain dust properties. Our results suggest that grain growth occurred in the ZZ Tau IRS disk, relative to sub-micron-sized interstellar medium. Planet formation in crescent with mm-sized pebbles might proceed more efficiently than in other regions with sub-millimeter-sized pebbles via pebble accretion scenarios.

24. PRODIGE – Envelope to Disk with NOEMA II. Small-scale temperature structure and a streamer feeding the SVS13A protobinary using CH3CN and DCN

T. -H. Hsieh, D. M. Segura-Cox, J. E. Pineda, P. Caselli, L. Bouscasse, R. Neri, A. Lopez-Sepulcre, M. T. Valdivia-Mena, M. J. Maureira, Th. Henning, G. V. Smirnov-Pinchukov, D. Semenov, Th. Möller, N. Cunningham, A. Fuente, S. Marino, A. Dutrey, M. Tafalla, E. Chapillon, C. Ceccarelli, B. Zhao ★ Aims. We present high sensitivity and high-spectral resolution NOEMA observations of the Class 0/I binary system SVS13A, composed of the low-mass protostars VLA4A and VLA4B with a separation of 90 au. VLA4A is undergoing an accretion burst that enriches the chemistry of the surrounding gas. This gives us an excellent opportunity to probe the chemical and physical conditions as well as the accretion process. Methods. We observe the (12K-11K) lines of CH3CN and CH313CN, the DCN (3-2) line, and the C18O (2-1) line toward SVS13A using NOEMA. Results. We find complex line profiles at disk scales which cannot be explained by a single component or pure Keplerian motion. By adopting two velocity components to model the complex line profiles, we find that the temperatures and densities are significantly different between these two components. This suggests that the physical conditions of the emitting gas traced via CH3CN can change dramatically within the circumbinary disk. In addition, combining our observations of DCN (3-2) with previous ALMA high-angular-resolution observations, we find that the binary system (or VLA4A) might be fed by an infalling streamer from envelope scales (700 au). If this is the case, this streamer contributes to the accretion of material onto the system with a rate of at least 1.4x10-6 Msun yr-1. Conclusions. We conclude that the CH3CN emission in SVS13A traces hot gas from a complex structure. This complexity might be affected by a streamer that is possibly infalling and funneling material into the central region.

25. Searching for converging flows of atomic gas onto a molecular cloud

Mark Heyer, Paul F. Goldsmith, Robert Simon, Rebeca Aladro, Oliver Ricken ★ We present new observations of [CII] fine structure line emission from an isolated molecular cloud using the upGREAT instrument onboard SOFIA. These data are analyzed together with archival CO=1-0 and HI 21 cm emission spectra to investigate the role of converging atomic gas flows in the formation of molecular clouds. Bright [CII] emission is detected throughout the mapped area that likely originates from photodissociation regions excited by UV radiation fields produced by newborn stars within the cloud. Upon spatial averaging of the [CII] spectra, we identify weak [CII] emission within velocity intervals where the HI 21 cm line is brightest; these are blue-shifted relative to velocities of the CO and bright [CII] emission by 4 km/s. The brightness temperatures, velocity dispersions, and alignment with HI 21 cm velocities connect this [CII] emission component to the cold, neutral atomic gas of the interstellar medium (CNM). We propose that this CNM feature is an accretion flow onto the far–side of the existing molecular cloud. The mass infall rate is 3.2x10**-4 Msun/yr. There is no direct evidence of a comparable red–shifted component in the [CII] or HI 21 cm spectral lines that would indicate the presence of a converging flow.

26. The Dissipation of the Solar Nebula Constrained by Impacts and Core Cooling in Planetesimals

Alison C. Hunt, Karen J. Theis, Mark Rehkämper, Gretchen K. Benedix, Rasmus Andreasen, Maria Schönbächler ★ Rapid cooling of planetesimal cores has been inferred for several iron meteorite parent bodies based on metallographic cooling rates, and linked to the loss of their insulating mantles during impacts. However, the timing of these disruptive events is poorly constrained. Here, we used the short-lived 107Pd / 107Ag decay system to date rapid core cooling by determining Pd-Ag ages for iron meteorites. We show closure times for the iron meteorites equate to cooling in the timeframe 7.8 to 11.7 Myr after CAI, and indicate that an energetic inner Solar System persisted at this time. This likely results from the dissipation of gas in the protoplanetary disk, after which the damping effect of gas drag ceases. An early giant planet instability between 5 and 14 Myr after CAI could have reinforced this effect. This correlates well with the timing of impacts recorded by the Pd Ag system for iron meteorites.

27. SPYGLASS III: The Fornax-Horologium Association and its Traceback History within the Austral Complex

Ronan Kerr, Adam L. Kraus, Simon J. Murphy, Daniel M. Krolikowski, Timothy R. Bedding, Aaron C. Rizzuto ★ The study of young associations is essential for building a complete record of local star formation processes. The Fornax-Horologium association (FH), including the χ^1 Fornacis cluster, represents one of the nearest young stellar populations to the Sun. This association has recently been linked to the Tuc-Hor, Carina, and Columba associations, building an extensive "Austral Complex" almost entirely within 150 pc. Using Gaia astrometry and photometry in addition to new spectroscopic observations, we perform the deepest survey of FH to date, identifying over 300 candidate members, nearly doubling the known population. By combining this sample with literature surveys of the other constituent populations, we produce a contiguous stellar population covering the entire Austral Complex, allowing the definitions of sub-populations to be re-assessed along with connections to external populations. This analysis recovers new definitions for FH, Tuc-Hor, Columba, and Carina, while also revealing a connection between the Austral complex and the Sco-Cen-affiliated Platais 8 cluster. This suggests that the Austral complex may be just a small component of a much larger and more diverse star formation event. Computing ages and tracing

stellar populations back to formation reveals two distinct nodes of cospatial and continuous formation in the Austral Complex, one containing Tuc-Hor, and the other containing FH, Carina, and Columba. This mirrors recent work showing similar structure elsewhere, suggesting that these nodes, which only emerge through the use of traceback, may represent the clearest discrete unit of local star formation, and a key building block needed to reconstruct larger star-forming events.

28. Characterising the high-mass star forming region IRAS 18144-1723 through methanol maser observations

Esraa Khafagy, khaled A. Edris, Osama M. Shalabiea, Anna Bartkiewicz, Anita M. S. Richards, Zainab Awad ★ We introduce a study of the massive star forming region IRAS 18144–1723 using observations of the 6.7 GHz methanol maser line. Such regions are opaque at short wavelengths but can be observed through radio emission lines. In this study we traced the kinematics of the source on milliarcsecond scales using the Multi-Element-Radio-Interferometer-Network (MERLIN). We found 52 maser spots in the LSR velocity range 45–52 km s^{-1}, near the centre of the previously-detected CO range of 21.3–71.3 km s^{-1}, lying within $\sim 0''.5$ of IRAS 18144–1723 'B', thought to be a young Class I protostar. Their distribution can be approximated as an ellipse, which, if it were rotating, would have its axis oriented south-east to north-west. The most probable morphology of the emitting regions is interaction between a disc and an outflow, possibly with a very large opening angle. The arcmin-scale CO outflow centred on source 'B' is oriented East-West, and the methanol masers do show the highest dispersion of velocity gradients in approximately this direction, so the kinematics are complex and suggest that more than one source may be responsible. We also tested kinematic models for a Keplerian disc or a simple bipolar outflow, but neither are compatible with the kinematics of the maser clumps and the characteristics of their internal velocities.

29. First spatially resolved Na I and He I transitions towards an MYSO. Finding new tracers for the gaseous star/disc interface

Evgenia Koumpia, M. Koutoulaki, W. -J. de Wit, R. D. Oudmaijer, A. J. Frost, S. L. Lumsden, J. M. Pittard ★ With steady observational advances, the formation of massive stars is being understood in more detail. Numerical models are converging on a scenario where accretion discs play a key role. Direct observational evidence of such discs at a few au scales is scarce, due to the rarity of such objects and the observational challenges, including the lack of adequate diagnostic lines in the near-IR. We present the analysis of K-band spectro-interferometric observations toward the Massive Young Stellar Object IRAS 13481-6124, which is known to host an accreting dusty disc. Using GRAVITY on the VLTI, we trace the crucial au-scales of the warm inner interface between the star and the accretion dusty disc. We detect and spatially resolve the Na I doublet and He I transitions towards an object of this class for the first time. The new observations in combination with our geometric models allowed us to probe the smallest au-scales of accretion/ejection around an MYSO. We find that Na I originates in the disc at smaller radii than the dust disc and is more compact than any of the other spatially resolved diagnostics (Brγ, He I, and CO). Our findings suggest that Na I can be a new powerful diagnostic line in tracing the warm star/disc accreting interface of forming (massive) stars, while the similarities between He I and Brγ point towards an accretion/ejection origin of He I

30. Protostellar collapse simulations in spherical geometry with dust coagulation and fragmentation

Ugo Lebreuilly, Valentin Vallucci-Goy, Vincent Guillet, Maxime Lombart, Pierre Marchand ★ We model the coagulation and fragmentation of dust grains during the protostellar collapse with our newly developed shark code. It solves the gas-dust hydrodynamics in a spherical geometry and the coagulation/fragmentation equation. It also computes the ionization state of the cloud and the Ohmic, ambipolar and Hall resistivities. We find that the dust size distribution evolves significantly during the collapse, large grain formation being controlled by the turbulent differential velocity. When turbulence is included, only ambipolar diffusion remains efficient at removing the small grains from the distribution, brownian motion is only efficient as a standalone process. The macroscopic gas-dust drift is negligible for grain growth and only dynamically significant near the first Larson core. At high density, we find that the coagulated distribution is unaffected by the initial choice of dust distribution. Strong magnetic fields are found to enhance the small grains depletion, causing an important increase of the ambipolar diffusion. This hints that the magnetic field strength could be regulated by the small grain population during the protostellar collapse. Fragmentation could be effective for bare silicates, but its modeling relies on the choice of ill-constrained parameters. It is also found to be negligible for icy grains. When fragmentation occurs, it strongly affects the magnetic resistivities profiles. Dust coagulation is a critical process that needs to be fully taken into account during the protostellar collapse. The onset and feedback of fragmentation remains uncertain and its modeling should be further investigated.

31. Dynamical mass measurements of two protoplanetary discs

G. Lodato, L. Rampinelli, E. Viscardi, C. Longarini, A. Inzquierdo, T. Paneque-Carreno, L. Testi, S. Facchini, A. Miotello, B. Veronesi, C. Hall ★ ALMA observations of line emission from planet forming discs have demonstrated to be an excellent tool to probe the internal disc kinematics, often revealing subtle effects related to important dynamical processes

occurring in them, such as turbulence, or the presence of planets, that can be inferred from pressure bumps perturbing the gas motion, or from detection of the planetary wake. In particular, we have recently shown for the case of the massive disc in Elias 2-27 how one can use such kind of observations to measure deviations from Keplerianity induced by the disc self-gravity, thus constraining the total disc mass with good accuracy and independently on mass conversion factors between the tracer used and the total mass. Here, we refine our methodology and extend it to two additional sources, GM Aur and IM Lup, for which archival line observations are available for both the 12CO and the 13CO line. For IM Lup, we are able to obtain a consistent disc mass of Mdisc=0.1 Msun, implying a disc-star mass ratio of 0.1 (consistent with the observed spiral structure in the continuum emission) and a gas/dust ratio of 65 (consistent with standard assumptions), with a systematic uncertainty by a factor 2 due to the different methods to extract the rotation curve. For GM Aur, the two lines we use provide slightly inconsistent rotation curves, that cannot be attributed only to a difference in the height of the emitting layer, nor to a vertical temperature stratification. Our best fit disc mass measurement is Mdisc=0.26Msun, implying a disc-star mass ratio of 0.35 and a gas/dust ratio of 130... ABRIDGED

32. Rapid Formation of Massive Planetary Cores in a Pressure Bump

Tommy Chi Ho Lau, Joanna Drążkowska, Sebastian M. Stammler, Tilman Birnstiel, Cornelis P. Dullemond ★

Models of planetary core growth by either planetesimal or pebble accretion are traditionally disconnected from the models of dust evolution and formation of the first gravitationally-bound planetesimals. The state-of-the-art models typically start with massive planetary cores already present. We aim to study the formation and growth of planetary cores in a pressure bump, motivated by the annular structures observed in protoplanetary disks, starting with sub-micron-sized dust grains. We connect the models of dust coagulation and drift, planetesimal formation in the streaming instability, gravitational interactions between planetesimals, pebble accretion, and planet migration, into one uniform framework. We find that planetesimals forming early at the massive end of the size distribution grow quickly dominantly by pebble accretion. These few massive bodies grow on the timescales of 100 000 years and stir the planetesimals formed later preventing the emergence of further planetary cores. Additionally, a migration trap occurs allowing for retention of the growing cores. Pressure bumps are favourable locations for the emergence and rapid growth of planetary cores by pebble accretion as the dust density and grain size are increased and the pebble accretion onset mass is reduced compared to a smooth-disk model.

33. A Census of the Taurus Star-forming Region and Neighboring Associations with Gaia

K. L. Luhman ★

I have used high-precision photometry and astrometry from the third data release of Gaia (DR3) to perform a survey for members of the Taurus star-forming region and young associations in its vicinity. This work has produced a new catalog of 532 adopted members of Taurus, which has only minor changes relative to the previous catalog from Esplin & Luhman 2019. I have used the Gaia astrometry to divide the Taurus members into 13 groups that have distinct kinematics. Meanwhile, I have identified 1378 candidate members of seven associations near Taurus. All of these associations have histograms of spectral types that peak near M5 (∼0.15 Msun), resembling other young populations in the solar neighborhood. For the Taurus groups and neighboring associations, I have estimated ages from their sequences of low-mass stars in Hertzsprung-Russell diagrams. Most of the Taurus groups have median ages of 1-3 Myr while the associations have ages ranging from 13 to 56 Myr. I have used mid-infrared photometry from the Wide-field Infrared Survey Explorer to search for excess emission from circumstellar disks among the candidate members of the associations. Disks are detected for 51 stars, 20 of which are reported for the first time in this work. Some recent studies have proposed that samples of older stars ($\geq$ 10 Myr) found in the vicinity of Taurus represent a distributed population that is associated with the Taurus cloud complex. However, I find that most of those stars have kinematics that are inconsistent with any relationship with Taurus.

34. Dependence of Chemical Abundance on the Cosmic Ray Ionization Rate in IC 348

Gan Luo, Zhi-Yu Zhang, Thomas G. Bisbas, Di Li, Ningyu Tang, Junzhi Wang, Ping Zhou, Pei Zuo, Nannan Yue, Jing Zhou, Lingrui Lin ★

Ions (e.g., H_3^+, H_2O^+) have been used extensively to quantify the cosmic-ray ionization rate (CRIR) in diffuse sightlines. However, measurements of CRIR in low-to-intermediate density gas environments are rare, especially when background stars are absent. In this work, we combine molecular line observations of CO, OH, CH, and HCO^+ in the star-forming cloud IC 348, and chemical models to constrain the value of CRIR and study the response of the chemical abundances distribution. The cloud boundary is found to have an A_V of approximately 4 mag. From the interior to the exterior of the cloud, the observed ^{13}CO line intensities drop by an order of magnitude. The calculated average abundance of ^{12}CO (assuming $^{12}C/^{13}C = 65$) is (1.2±0.9) $\times 10^{-4}$, which increases by a factor of 6 from the interior to the outside regions. The average abundance of CH ($3.3\pm0.7 \times 10^{-8}$) is in good agreement with previous findings in diffuse and translucent clouds ($A_V <$ 5 mag). However, we did not find a decline in CH abundance in regions of high extinction ($A_V \simeq 8$ mag) as previously reported in Taurus. By comparing the observed molecular abundances and chemical models, we find a decreasing trend of CRIR as A_V increases. The inferred CRIR of $\zeta_{cr} = (4.7\pm1.5) \times 10^{-16}$ s^{-1} at low A_V is consistent with H_3^+ measurements toward two nearby massive stars.

35. Mid-infrared time-domain study of recent dust production events in the extreme debris disc of TYC 4209-1322-1

A. Moór, P. Ábrahám, Á. Kóspál, K. Y. L. Su, G. H. Rieke, G. Cataldi, A. Bódi, Zs. Bognár, B. Cseh, G. Csörnyei, N. Egei, A. Farkas, O. Hanyecz, B. Ignácz, Cs. Kalup, R. Könyves-Tóth, L. Kriskovics, L. Mészáros, A. Pál, A. Ordasi, K. Sárneczky, B. Seli, Á. Sódor, R. Szakáts, J. Vinkó, G. Zsidi ★ Extreme debris discs are characterized by unusually strong mid-infrared excess emission, which often proves to be variable. The warm dust in these discs is of transient nature and is likely related to a recent giant collision occurring close to the star in the terrestrial region. Here we present the results of a 877 days long, gap-free photometric monitoring performed by the Spitzer Space Telescope of the recently discovered extreme debris disc around TYC 4209-1322-1. By combining these observations with other time-domain optical and mid-infrared data, we explore the disc variability of the last four decades with particular emphasis on the last 12 yr. During the latter interval the disc showed substantial changes, the most significant was the brightening and subsequent fading between 2014 and 2018 as outlined in WISE data. The Spitzer light curves outline the fading phase and a subsequent new brightening of the disc after 2018, revealing an additional flux modulation with a period of 39 days on top of the long-term trend. We found that all these variations can be interpreted as the outcome of a giant collision that happened at an orbital radius of 0.3 au sometime in 2014. Our analysis implies that a collision on a similar scale could have taken place around 2010, too. The fact that the disc was already peculiarly dust rich 40 yr ago, as implied by IRAS data, suggests that these dust production events belong to a chain of large impacts triggered by an earlier even more catastrophic collision.

36. Investigating the hot molecular core, G10.47+0.03: A pit of nitrogen-bearing complex organic molecules

Suman Kumar Mondal, Wasim Iqbal, Prasanta Gorai, Bratati Bhat, Valentine Wakelam, Ankan Das ★ Recent observations have shown that Nitrogen-bearing complex organic species are present in large quantities in star-forming regions. Thus, investigating the N-bearing species in a hot molecular core, such as G10.47+0.03, is crucial to understanding the molecular complexity in star-forming regions. They also allow us to investigate the chemical and physical processes that determine the many phases during the structural and chemical evolution of the source in star-forming regions. The aim of this study is to investigate the spatial distribution and the chemical evolution states of N-bearing complex organic molecules in the hot core G10.47+0.03. We used the ALMA archival data of the hot molecular core G10.47+0.03. The extracted spectra were analyzed assuming LTE. Furthermore, robust methods such as MCMC and rotational diagram methods are implemented for molecules for which multiple transitions were identified to constrain the temperature and column density. Finally, we used the Nautilus gas-grain code to simulate the nitrogen chemistry in the hot molecular core. We carried out both 0D and 1D simulations of the source and compared with observational results. We report various transitions of nitrogen-bearing species (NH2CN, HC3N, HC5N, C2H3CN, C2H5CN, and H2NCH2CN) together with some of their isotopologues and isomers. Besides this, we also report the identification of CH3CCH and one of its isotopologues. The emissions originating from vinyl cyanide, ethyl cyanide, cyanoacetylene, and cyanamide are compact, which could be explained by our astrochemical modeling. Our 0D model shows that the chemistry of certain N-bearing molecules can be very sensitive to initial local conditions such as density or dust temperature. In our 1D model, simulated higher abundances of species such as HCN, HC3N, and HC5N toward the inner shells of the source confirm the observational findings.

37. Imaging of HH80-81 jet in the NIR shock tracers H_2 and [Fe II]

Sreelekshmi Mohan, Sarita Vig, Watson P. Varricatt, Anandmayee Tej ★ The HH80-81 system is one of the most powerful jets driven by a massive protostar. We present new near-infrared (NIR) line imaging observations of the HH80-81 jet in the H_2 (2.122 μm) and [Fe II] (1.644 μm) lines. These lines trace not only the jet close to the exciting source but also the knots located farther away. We have detected nine groups of knot-like structures in the jet including HH80 and HH81 spaced $0.2 - 0.9$ pc apart. The knots in the northern arm of the jet show only [Fe II] emission closer to the exciting source, a combination of [Fe II] and H_2 at intermediate distances, and solely H_2 emission farther outwards. Towards the southern arm, all the knots exhibit both H_2 and [Fe II] emission. The nature of the shocks is inferred by assimilating the NIR observations with radio and X-ray observations from literature. In the northern arm, we infer the presence of strong dissociative shocks, in the knots located close to the exciting source. The knots in the southern arm that include HH80 and HH81 are explicable as a combination of strong and weak shocks. The mass-loss rates of the knots determined from [Fe II] luminosities are in the range $\sim 3.0 \times 10^{-7} - 5.2 \times 10^{-5}$ $M_\odot$ yr^{-1}, consistent with those from massive protostars. Towards the central region, close to the driving source of the jet, we have observed various arcs in H_2 emission which resemble bow shocks, and strings of H_2 knots which reveal traces of multiple outflows.

38. The complex organic molecular content in the L1517B starless core

Andrés Megías, Izaskun Jiménez-Serra, Jesús Martín-Pintado, Anton I. Vasyunin, Silvia Spezzano, Paola Caselli, Giuliana Cosentino, Serena Viti ★ Recent observations of the pre-stellar core L1544 and the younger starless core L1498 have revealed that complex organic molecules (COMs) are enhanced in the gas phase toward their outer and intermediate-

density shells. Our goal is to determine the level of chemical complexity toward the starless core L1517B, which seems younger than L1498, and compare it with the other two previously studied cores to see if there is a chemical evolution within the cores. We have carried out 3 mm high-sensitivity observations toward two positions in the L1517B starless core: the core's centre and the position where the methanol emission peaks (at a distance of ∼5000 au from the core's centre). Our observations reveal that a lower number of COMs and COM precursors are detected in L1517B with respect to L1498 and L1544, and also show lower abundances. Besides methanol, we only detected H_2CCO, CH_3CHO, CH_3CN, CH_3NC, HCCCN, and HCCNC. Their measured abundances are ∼3 times larger toward the methanol peak than toward the core's centre, mimicking the behaviour found toward the more evolved cores L1544 and L1498. We propose that the differences in the chemical complexity observed between the three studied starless cores are a consequence of their evolution, with L1517B being the less evolved one, followed by L1498 and L1544. Chemical complexity in these cores seems to increase over time, with N-bearing molecules forming first and O-bearing COMs forming at a later stage as a result of the catastrophic depletion of CO.

39. Importance of source structure on complex organics emission III. Effect of disks around massive protostars

P. Nazari, B. Tabone, G. P. Rosotti ★ Complex organic molecules are only detected toward a fraction of high-mass protostars. The goal of this work is to investigate whether high-mass disks can explain the lack of methanol emission from some massive protostellar systems. We consider an envelope-only and an envelope-plus-disk model and use RADMC-3D to calculate the methanol emission. High and low millimeter (mm) opacity dust are considered for both models separately and the methanol abundance is parameterized. Viscous heating is included due to the high accretion rates of these objects in the disk. In contrast with low-mass protostars, the presence of a disk does not significantly affect the temperature structure and methanol emission. The shadowing effect of the disk is not as important for high-mass objects and the disk mid-plane is hot because of viscous heating, which is effective due to the high accretion rates. Consistent with observations of infrared absorption lines toward high-mass protostars, we find a vertical temperature inversion, i.e. higher temperatures in the disk mid-plane than the disk surface, at radii $<$ 50au for the models with $L = 10^4$ $L_\odot$ and large mm opacity dust as long as the envelope mass is $>$550 $M_\odot$. The large observed scatter in methanol emission from massive protostars can be mostly explained toward lower luminosity objects with the envelope-plus-disk models including low and high mm opacity dust. The methanol emission variation toward sources with high luminosities cannot be explained by models with or without a disk. However, the L/M of these objects suggest that they could be associated with hypercompact/ultracompact HII regions. Therefore, the low methanol emission toward the high-luminosity sources can be explained by them hosting an HII region where methanol is absent.

40. Turbulence, Coherence and Collapse: Three Phases for Core Evolution

Stella S. R. Offner, Josh Taylor, Carleen Markey, Hope How-Huan Chen, Jaime E. Pineda, Alyssa A. Goodman, Andreas Burkert, Adam Ginsburg, Spandan Choudhury ★ We study the formation, evolution and collapse of dense cores by tracking structures in a magnetohydrodynamic simulation of a star-forming cloud. We identify cores using the dendrogram algorithm and utilize machine learning techniques, including Neural Gas prototype learning and Fuzzy c-means clustering, to analyze the density and velocity dispersion profiles of cores together with six bulk properties. We produce a 2-d visualization using a Uniform Manifold Approximation and Projection (UMAP), which facilitates the connection between physical properties and three partially-overlapping phases: i) unbound turbulent structures (Phase I), ii) coherent cores that have low turbulence (Phase II), and iii) bound cores, many of which become protostellar (Phase III). Within Phase II we identify a population of long-lived coherent cores that reach a quasi-equilibrium state. Most prestellar cores form in Phase II and become protostellar after evolving into Phase III. Due to the turbulent cloud environment, the initial core properties do not uniquely predict the eventual evolution, i.e., core evolution is stochastic, and cores follow no one evolutionary path. The phase lifetimes are $1.0\pm0.1\times10^5$ yr, $1.3\pm0.2\times10^5$ yr, and $1.8\pm0.3\times10^5$ yr for Phase I, II, and III, respectively. We compare our results to NH_3 observations of dense cores. Known coherent cores predominantly map into Phase II, while most turbulent pressure-confined cores map to Phase I or III. We predict that a significant fraction of observed starless cores have unresolved coherent regions and that $\gtrsim$ 20% of observed starless cores will not form stars. Measurements of core radial profiles, in addition to the usual bulk properties, will enable more accurate predictions of core evolution.

41. Backscattering and Line Broadening in Orion

C. R. O'Dell, G. J. Ferland, J. E. Mendez-Delgado ★ Examination of emission lines in high-velocity resolution optical spectra of the Orion Nebula confirms that the velocity component on the red wing of the main ionization front emission line is due to backscattering in the Photon Dominated Region. This scattered light component has a weak wavelength dependence that is consistent with either general interstellar medium particles or particles in the foreground of the Orion Nebula Cluster. An anomalous line-broadening component that has been known for 60+ years is characterized in unprecedented detail. Although this extra broadening may be due to turbulence along the line-of-sight of our spectra, we explore the possibility that it is due to Alvén waves in conditions where the ratio of magnetic and thermal energies are about equal and constant throughout the ionized gas.

42. A Circumplanetary Dust Ring May Explain the Extreme Spectral Slope of the 10 Myr Young Exoplanet K2-33b

Kazumasa Ohno, Pa Chia Thao, Andrew W. Mann, Jonathan J. Fortney ★ Young exoplanets are attractive targets for atmospheric characterization to explore the early phase of planetary evolution and the surrounding environment. Recent observations of the 10 Myr young Neptune-sized exoplanet K2-33b revealed that the planet's transit depth drastically decreases from the optical to near-infrared wavelengths. Thao et al. (2022) suggested that a thick planetary haze and/or stellar spots may be the cause; however, even the best-fit model only barely explains the data. Here, we propose that the peculiar transmission spectrum may indicate that K2-33b possess a circumplanetary dust ring, an analog of Jupiter's dust ring. We demonstrate that the ring could produce a steep slope in the transmission spectrum even if its optical depth is as low as $\sim 10^{-2}$. We then apply a novel joint atmosphere-ring retrieval to K2-33b and find that the ring scenario could well explain the observed spectrum for various possible ring compositions. Importantly, the dust ring also exhibits prominent absorption features of ring particles around $\sim$10 μm, whose shape and strength depend on the composition of the ring. Thus, future observations by JWST-MIRI would be able to test not only the ring hypothesis but also, if it indeed exists, to constrain the composition of the ring – providing a unique opportunity to explore the origins of the dust ring around its parent planet, soon after the planetary system's formation.

43. Peering into the Young Planetary System AB Pic. Atmosphere, Orbit, Obliquity & Second Planetary Candidate

P. Palma-Bifani, G. Chauvin, M. Bonnefoy, P. M. Rojo, S. Petrus, L. Rodet, M. Langlois, F. Allard, B. Charnay, C. Desgrange, D. Homeier, A. -M. Lagrange, J. -L. Beuzit, P. Baudoz, A. Boccaletti, A. Chomez, P. Delorme, S. Desidera, M. Feldt, C. Ginski, R. Gratton, A. -L. Maire, M. Meyer, M. Samland, I. Snellen, A. Vigan, Y. Zhang ★ We aim to revisit the system AB Pic which has a known companion at the exoplanet/ brown-dwarf boundary. We based this study on a rich set of observations to investigate the companion's orbit and atmosphere. We composed a spectrum of AB Pic b merging archival VLT/SINFONI K-band data, with published spectra at J and H-band (SINFONI) and Lp-band (Magellan-AO), and photometric measurements (HST and Spitzer). We modeled the spectrum with ForMoSA, based on two atmospheric models: ExoREM and BT-SETTL13. We determined the orbital properties of b fitting the astrometric measurements from NaCo (2003 and 2004) and SPHERE (2015). The orbital solutions favor a semi-major axis of $\sim$190au viewed edge-on. With Exo-REM, we derive a T_{eff} of 1700$\pm$50K and surface gravity of 4.5$\pm$0.3dex, consistent with previous works, and we report for the first time a C/O ratio of 0.58$\pm$0.08 ($\sim$solar). The posteriors are sensitive to the wavelength interval and the family of models used. Given the 2.1hr rotation period and our vsin(i) of $\sim$73km/s, we estimate for the first time the true obliquity to be $\sim$45 or $\sim$135deg, indicating a significant misalignment between the planet's spin and orbit orientations. Finally, the existence of a proper motion anomaly between the Hipparcos and Gaia eDR3 compared to our SPHERE detection limits and adapted radial velocity limits indicate the existence of a $\sim$6M_{Jup} inner planet orbiting from 2 to 10au (40-200mas). The possible existence of an inner companion, together with the likely miss-alignment of the spin axis orientation, strongly favor a formation path by gravitational instability or core accretion within a disk closer inside followed by dynamical interactions. Confirmation and characterization of planet c and access to a broader wavelength coverage for planet b will be essential to probe the uncertainties associated with the parameters.

44. Photometric and spectroscopic study of the EXor-like eruptive young star Gaia19fct

Sunkyung Park, Ágnes Kóspál, Péter Ábrahám, Fernando Cruz-Sáenz de Miera, Eleonora Fiorellino, Michał Siwak, Zsófia Nagy, Teresa Giannini, Roberta Carini, Zsófia Marianna Szabó, Jeong-Eun Lee, Jae-Joon Lee, Fabrizio Vitali, Mária Kun, Borbála Cseh, Máté Krezinger, Levente Kriskovics, András Ordasi, András Pál, Róbert Szakáts, Krisztián Vida, József Vinkó ★ Gaia19fct is one of the Gaia-alerted eruptive young stars that has undergone several brightening events. We conducted monitoring observations using multi-filter optical and near-infrared photometry, as well as near-infrared spectroscopy, to understand the physical properties of Gaia19fct and investigate whether it fits into the historically defined two classes. We present the analyses of light curves, color variations, spectral lines, and CO modeling. The light curves show at least five brightening events since 2015, and the multi-filter color evolutions are mostly gray. The gray evolution indicates that bursts are triggered by mechanisms other than extinction. Our near-infrared spectra exhibit both absorption and emission lines and show time-variability throughout our observations. We found lower rotational velocity and lower temperature from the near-infrared atomic absorption lines than from the optical lines, suggesting that Gaia19fct has a Keplerian rotating disk. The CO overtone features show a superposition of absorption and emission components, which is unlike other young stellar objects. We modeled the CO lines, and the result suggests that the emission and absorption components are formed in different regions. We found that although Gaia19fct exhibits characteristics of both types of eruptive young stars, FU Orionis-type objects (FUors) and EX Lupi-type objects (EXors), it shows more similarity with EXors in general.

45. Three-dimensional evolution of radiative circumbinary discs: the size and shape of the inner cavity

Arnaud Pierens, Richard Nelson ★ The evolution of circumbinary discs and planets is often studied using two-dimensional (2D) numerical simulations, although recent work suggests that 3D effects may significantly alter the structure of the inner cavity created by the binary. In this study, we present the results of 3D hydrodynamical simulations of circumbinary discs that orbit around analogues of the Kepler-16 and Kepler-34 systems, including the effect of stellar heating and radiative cooling on the thermal disc structure. We find that compared to their 2D counterparts, the structures of the cavities in 3D circumbinary disc models appear to reach a quasi-stationary state more rapidly, and in a subset of our runs the evidence for this is unambiguous. Furthermore, the sizes and eccentricities of the inner cavity are smaller in 3D compared to 2D. We attribute this difference to enhanced spiral wave dissipation in disc regions above the midplane, where the cooling time is of the order of the dynamical timescale, resulting in smaller inner cavity sizes in 3D disc models. Our results suggest that migrating planets should park closer to the central binary in 3D models of circumbinary discs, and point to the importance of including the 3D structure when simulating circumbinary discs and planets.

46. Accretion process, magnetic fields, and apsidal motion in the pre-main sequence binary DQ Tau

Kim Pouilly, Oleg Kochukhov, Ágnes Kóspál, Axel Hahlin, Andres Carmona, Péter Ábrahám ★ Classical T Tauri stars (CTTSs) are young stellar objects that accrete materials from their accretion disc influenced by their strong magnetic field. The magnetic pressure truncates the disc at a few stellar radii and forces the material to leave the disc plane and fall onto the stellar surface by following the magnetic field lines. However, this global scheme may be disturbed by the presence of a companion interacting gravitationally with the accreting component. This work is aiming to study the accretion and the magnetic field of the tight eccentric binary DQ Tau, composed of two equal-mass (~ 0.6 $M_\odot$) CTTSs interacting at different orbital phases. We investigated the variability of the system using a high-resolution spectroscopic and spectropolarimetric monitoring performed with ESPaDOnS at the CFHT. We provide the first ever magnetic field analysis of this system, the Zeeman-Doppler imaging revealed a stronger magnetic field for the secondary than the primary (1.2 kG and 0.5 kG, respectively), but the small-scale fields analysed through Zeeman intensification yielded similar strengths (about 2.5 kG). The magnetic field topology and strengths are compatible with the accretion processes on CTTSs. Both components of this system are accreting, with a change of the main accretor during the orbital motion. In addition, the system displays a strong enhancement of the mass accretion rate at periastron and apastron. We also discovered, for the first time in this system, the apsidal motion of the orbital ellipse.

47. Differences in chemical evolution between isolated and embedded prestellar cores

F. D. Priestley, A. P. Whitworth, E. Fogerty ★ Models of prestellar cores often assume that the cores are isolated from their environment - material outside the core boundary plays no role in the subsequent evolution. This is unlikely to be the case in reality, where cores are located within hierarchically substructured molecular clouds. We investigate the dynamical and chemical evolution of prestellar cores, modelled as Bonnor-Ebert spheres, and show that the density of the ambient medium has a large impact on the resulting chemical properties of the cores. Models embedded in high-density, low-temperature surroundings have greatly enhanced abundances of several molecules, such as CO and CS, compared to models with more diffuse surroundings, corresponding to relatively isolated cores. The predicted intensities and profile shapes of molecular lines are also affected. The density of the ambient medium has a stronger effect on the chemical evolution than whether the cores are initially in or out of equilibrium. This suggests that the impact of environment cannot be neglected when modelling chemistry in prestellar cores; the results of these models are highly sensitive to the assumptions made about the core surroundings.

48. A Massive Star is Born: How Feedback from Stellar Winds, Radiation Pressure, and Collimated Outflows Limits Accretion onto Massive Stars

Anna L. Rosen ★ Massive protostars attain high luminosities as they are actively accreting and the radiation pressure exerted on the gas in the star's atmosphere may launch isotropic high-velocity winds. These winds will collide with the surrounding gas producing shock-heated ($T \sim 10^7$ K) tenuous gas that adiabatically expands and pushes on the dense gas that may otherwise be accreted. We present a suite of 3D radiation-magnetohydrodynamic simulations of the collapse of massive prestellar cores and include radiative feedback from the stellar and dust-reprocessed radiation fields, collimated outflows, and, for the first time, isotropic stellar winds to model how these processes affect the formation of massive stars. We find that winds are initially launched when the massive protostar is still accreting and its wind properties evolve as the protostar contracts to the main-sequence. Wind feedback drives asymmetric adiabatic wind bubbles that have a bipolar morphology because the dense circumstellar material pinches the expansion of the hot shock-heated gas. We term this the "wind tunnel effect." If the core is magnetized, wind feedback is less efficient at driving adiabatic wind bubbles initially because magnetic tension delays their growth. We find that wind feedback eventually quenches accretion onto $\sim$30 $M_\odot$ protostars that form from the collapse of the isolated cores simulated here. Hence, our results suggest that $\gtrsim$30 $M_\odot$ stars likely require larger-scale dynamical inflows from their host cloud to overcome wind feedback. Additionally, we discuss the implications of observing adiabatic wind bubbles with

Chandra while the massive protostars are still highly embedded.

49. The core population and kinematics of a massive clump at early stages: an ALMA view

E. Redaelli, S. Bovino, P. Sanhueza, K. Morii, G. Sabatini, P. Caselli, A. Giannetti, S. Li ★ High-mass star formation theories make distinct predictions on the properties of the prestellar seeds of high-mass stars. Observations of the early stages of high-mass star formation can provide crucial constraints, but they are challenging and scarce. We investigate the properties of the prestellar core population embedded in the high-mass clump AGAL014.492-00.139, and we study the kinematics at the clump and the clump-to-core scales. We have analysed an extensive dataset acquired with the ALMA interferometer. Applying a dendrogram analysis to the Band o-H_2D^+ data, we identified 22 cores. We have fitted their average spectra in local-thermodinamic-equilibrium conditions, and we analysed their continuum emission at 0.8 mm. The cores have transonic to mildly supersonic turbulence levels and appear mostly low-mass, with $M_{\rm core} < 30\,{\rm M}_\odot$. Furthermore, we have analysed Band 3 observations of the N_2H^+ (1-0) transition, which traces the large scale gas kinematics. Using a friend-of-friend algorithm, we identify four main velocity coherent structures, all of which are associated with prestellar and protostellar cores. One of them presents a filament-like structure, and our observations could be consistent with mass accretion towards one of the protostars. In this case, we estimate a mass accretion rate of $\dot{M}_{\rm acc} \approx 2 \times 10^{-4}\,{\rm M}_\odot\,{\rm yr}^{-1}$. Our results support a clump-fed accretion scenario in the targeted source. The cores in prestellar stage are essentially low-mass, and they appear subvirial and gravitationally bound, unless further support is available for instance due to magnetic fields.

50. A large (1 pc) contracting envelope around the prestellar core L1544

E. Redaelli, A. Chacón-Tanarro, P. Caselli, M. Tafalla, J. E. Pineda, S. Spezzano, O. Sipilä ★ Prestellar cores, the birthplace of Sun-like stars, form from the fragmentation of the filamentary structure that composes molecular clouds, from which they must inherit at least partially the kinematics. Furthermore, when they are on the verge of gravitational collapse, they show signs of subsonic infall motions. How extended these motions are, which depends on how the collapse occurs, remains largely unknown. We want to investigate the kinematics of the envelope that surrounds the prototypical prestellar core L1544, studying the cloud-core connection. To our aims, we observed the HCO^+(1-0) transition in a large map. HCO+ is expected to be abundant in the envelope, making it an ideal probe of the large-scale kinematics in the source. We modelled the spectrum at the dust peak by means of a non local-thermodynamical-equilibrium radiative transfer. In order to reproduce the spectrum at the dust peak, a large (~ 1 pc) envelope is needed, with low density (tens of $\rm cm^{-3}$ at most) and contraction motions, with an inward velocity of $\approx 0.05\,{\rm km\,s^{-1}}$. We fitted the data cube using the Hill5 model, which implements a simple model for the optical depth and excitation temperature profiles along the line-of-sight, in order to obtain a map of the infall velocity. This shows that the infall motions are extended, with typical values in the range $0.1 - 0.2\,{\rm km\,s^{-1}}$. Our results suggest that the contraction motions extend in the diffuse envelope surrounding the core, which is consistent with recent magnetic field measurements in the source, which showed that the envelope is magnetically supercritical.

51. Interpreting molecular hydrogen and atomic oxygen line emission of T Tauri disks with photoevaporative disk-wind models

Ch. Rab, M. Weber, T. Grassi, B. Ercolano, G. Picogna, P. Caselli, W. -F. Thi, I. Kamp, P. Woitke ★ Winds in protoplanetary disks play an important role in their evolution and dispersal. However, what physical process is driving the winds is still unclear (i.e. magnetically vs thermally driven), and can only be understood by directly confronting theoretical models with observational data. We use hydrodynamic photoevaporative disk-wind models and post-process them with a thermo-chemical model to produce synthetic observables for the o-H_2 at 2.12 micron and [OI] at 0.63 micron spectral lines and directly compare the results to a sample of observations. Our photoevaporative disk-wind model is consistent with the observed signatures of the blueshifted narrow low-velocity component (NLVC), which is usually associated with slow disk winds, for both tracers. Only for one out of seven targets that show blueshifted NLVCs does the photoevaporative model fail to explain the observed line kinematics. Our results also indicate that interpreting spectral line profiles by simple methods, such as the thin-disk approximation, to determine the line emitting region can yield misleading conclusions. The photoevaporative disk-wind models are largely consistent with the studied observational data set, but it is not possible to clearly discriminate between different wind-driving mechanisms. Further improvements to the models, such as consistent modelling of the dynamics and chemistry and detailed modelling of individual targets would be beneficial. Furthermore, a direct comparison of magnetically driven disk-wind models to the observational data set is necessary in order to determine whether or not spatially unresolved observations of multiple wind tracers are sufficient to discriminate between theoretical models.

52. Stellar Properties for a Comprehensive Collection of Star Forming Regions in the SDSS APOGEE-2 Survey

Carlos G. Román-Zúñiga, Marina Kounkel, Jesús Hernández, Karla Peña Ramírez, Ricardo López-Valdivia, Kevin R. Covey, Amelia M. Stutz, Alexandre Román-López, Hunter Campbell, Eliott Khilfeh, Mauricio Tapia, Guy S. Stringfellow, Juan José Downes, Keivan G. Stassun, Dante Minniti, Amelia Bayo, Jinyoung Serena Kim, Genaro Suárez, Jason Ybarra, José G. Fernández-Trincado, Penélope Longa-Peña, Valeria Ramírez-Preciado, Javier Serna, Richard R. Lane, D. A. García-Hernández, Rachael L. Beaton, Dmitry Bizyaev, Kaike Pan ★ The Sloan Digital Sky Survey IV (SDSS-IV) APOGEE-2 primary science goal was to observe red giant stars throughout the Galaxy to study its dynamics, morphology, and chemical evolution. The APOGEE instrument, a high-resolution 300 fiber H-band (1.55-1.71 micron) spectrograph, is also ideal to study other stellar populations in the Galaxy, among which are a number of star forming regions and young open clusters. We present the results of the determination of six stellar properties (T_{eff}, $\log g$, [Fe/H], $L/L_{\odot}$, $M/M_{\odot}$, and ages) for a sample that is composed of 3360 young stars, of sub-solar to super-solar types, in sixteen Galactic star formation and young open cluster regions. Those sources were selected by using a clustering method that removes most of the field contamination. Samples were also refined by removing targets affected by various systematic effects of the parameter determination. The final samples are presented in a comprehensive catalog that includes all six estimated parameters. This overview study also includes parameter spatial distribution maps for all regions and Hertzprung-Russell ($L/L_{\odot}$ vs. T_{eff}) diagrams. This study serves as a guide for detailed studies on individual regions, and paves the way for the future studies on the global properties of stars in the pre-main sequence phase of stellar evolution using more robust samples.

53. Accretion variability in RU Lup

Camille Stock, Pauline McGinnis, Alessio Caratti o Garatti, Antonella Natta, Tom P. Ray ★ The process of accretion in classical T Tauri stars (CTTSs) has been observed to vary on different timescales. Studying this variability is vital to understanding a star's evolution and provides insight into the complex processes at work within. Understanding the dichotomy between continuum veiling and emission line veiling is integral to accurately measuring the amount of veiling present in stellar spectra. Here, 15 roughly consecutive nights of optical spectroscopic data from the spectropolarimeter ESPaDOnS are utilised to characterise the short-term accretion activity in the CTTS, RU Lup, and investigate its relationship with the veiling in the LiI 6707A absorption line. The accretion-tracing HI Balmer series emission lines were studied and used to obtain the accretion luminosity (Lacc) and mass accretion rate (Macc) for each night, which vary by a factor of 2 between the brightest and dimmest nights. We also measured the veiling using multiple photospheric absorption lines (NaI 5688A, MnI 6021A, and LiI 6707A) for each night. We find the LiI 6707A line provides measurements of veiling that produce a strong, positive correlation with Lacc in the star. When corrected for Li depletion, the average veiling measured in the LiI 6707A line is $r_{LiI(avg)}$ ∼3.25±0.20, which is consistent with the other photospheric lines studied (r_avg ∼3.28±0.65). We measured short timescale variability in the Lacc and Macc that are intrinsic and not due to geometric effects. Upon comparing the changes in veiling and Lacc, we find a strong, positive correlation. This study provides an example of how this correlation can be used as a tool to determine whether a measured variability is due to extinction or an intrinsic change in accretion. As the determination of veiling is an independent process from measuring Lacc, their relationship allows further exploration of accretion phenomena in young stars.

54. High-contrast Imaging around a 2 Myr-old CI Tau with a Close-in Gas Giant

Toshinori Shimizu, Taichi Uyama, Yasunori Hori, Motohide Tamura, Nicole Wallack ★ Giant planets around young stars serve as a clue to unveiling their formation history and orbital evolution. CI Tau is a 2 Myr-old classical T-Tauri star hosting an eccentric hot Jupiter, CI Tau b. The standard formation scenario of a hot Jupiter predicts that planets formed further out and migrated inward. A high eccentricity of CI Tau b may be suggestive of high-e migration due to secular gravitational perturbations by an outer companion. Also, ALMA 1.3 mm-continuum observations show that CI Tau has at least three annular gaps in which unseen planets may exist. We present high-contrast imaging around CI Tau taken from Keck/NIRC2 L'-band filter and vortex coronagraph that allows us to search for an outer companion. We did not detect any outer companion around CI Tau from angular differential imaging (ADI) using two deep imaging data sets. The detection limits from ADI-reduced images rule out the existence of an outer companion beyond ~ 30 au that can cause the Kozai-Lidov migration of CI Tau b. Our results suggest that CI Tau b may have experienced Type II migration from $\lesssim 2$ au in Myrs. We also confirm that no planets with $\geq 2-4\,M_{\rm Jup}$ are hidden in two outer gaps.

55. The link between infall location, early disc size, and the fraction of self-gravitationally fragmenting discs

O. Schib, C. Mordasini, R. Helled ★ Many protoplanetary discs are self-gravitating early in their lives. If they fragment under their own gravity, they form bound gaseous clumps which may evolve to become giant planets. Today, the fraction of discs that undergo fragmentation, and the frequency of conditions that may lead to giant planet formation via gravitational instability, is still unknown. We perform a population synthesis of discs from formation to dispersal. In varying the infall

radius, we study the relationship of the early disc size with fragmentation. Furthermore, we investigate how stellar accretion heating affects the fragmentation fraction. We find that discs fragment only if they become sufficiently large early in their lives. This size depends sensitively on where mass is added to the discs during the collapse of their parent molecular cloud core. By choosing intermediate infall locations leading to a synthetic disc size distribution that is in agreement with the observed one, we find a fragmentation fraction between 0.1 and 11%, depending on the efficiency of stellar accretion heating of the discs. We conclude that the early disc size is mainly determined by the infall location during the collapse of the molecular cloud core and controls the population-wide frequency of fragmentation. Stellar accretion heating plays an important role for fragmentation and must be studied further. Our work is an observationally-informed step towards a prediction of the frequency of giant planet formation by gravitational instability. Upcoming observations and theoretical studies will deepen our understanding of the formation and early evolution of discs, eventually allowing to understand how infall, disc morphology, giant planet formation via gravitational instability, and the observed extrasolar planet population are linked.

56. A Low-Mass Pre-Main-Sequence Eclipsing Binary in Lower Centaurus Crux Discovered with TESS

Keivan G. Stassun, Guillermo Torres, Marina Kounkel, Dax L. Feliz, Luke G. Bouma, Steve B. Howell, Crystal L. Gnilka, E. Furlan ★ We report the discovery of 2M1222-57 as a low-mass, pre-main-sequence (PMS) eclipsing binary (EB) in the Lower Centaurus Crux (LCC) association for which, using Gaia parallaxes and proper motions with a neural-net age estimator, we determine an age of 16.2±2.2 Myr. The broadband spectral energy distribution (SED) shows clear excess at 10 um indicative of a circumbinary disk, and new speckle-imaging observations reveal a faint, tertiary companion separated by 100 AU. H-alpha emission is modulated on the orbital period, consistent with theoretical models of orbitally pulsed accretion streams reaching from the inner disk edge to the central stars. From a joint analysis of spectroscopically determined radial velocities and TESS light curves, together with additional tight constraints provided by the SED and the Gaia parallax, we measure masses for the eclipsing stars of 0.74 Msun and 0.67 Msun; radii of 0.98 Rsun and 0.94 Rsun; and effective temperatures of 3750 K and 3645 K. The masses and radii of both stars are measured to an accuracy of 1%. The measured radii are inflated, and the temperatures suppressed, relative to predictions of standard PMS evolutionary models at the age of LCC; also, the Li abundances are 2 dex less depleted than predicted by those models. However, models that account for the global and internal effects of surface magnetic fields are able to simultaneously reproduce the measured radii, temperatures, and Li abundances at an age of 17.0±0.5 Myr. Altogether, the 2M1222-57 system presents very strong evidence that magnetic activity in young stars alters both their global properties and the physics of their interiors.

57. Effective dust growth in laminar circumplanetary discs with magnetic wind-driven accretion

Yuhito Shibaike, Shoji Mori ★ It has been considered that large satellites around gas planets form in-situ circumplanetary discs (CPDs). However, dust particles supplied into CPDs drift toward the central planets before they grow into satellitesimals, building blocks of the satellites. We investigate the dust growth in laminar CPDs with magnetic wind-driven accretion. In such laminar discs, dust particles can settle onto the mid-plane and grow large by mutual collision more efficient than in classical turbulent CPDs. First, we carry out 3D local MHD simulations of a CPD including all the nonideal MHD effects (Ohmic resistivity, Hall effect and ambipolar diffusion). We investigate if the disk accretion can be governed by magnetic wind-driven accretion and how laminar the disc can be, in a situation where the magnetic disc wind can be launched from the disc. Second, we model 1D steady CPDs consistent with the results of the MHD simulations and calculate the steady radial distributions of the dust profiles in the modeled discs, taking account of the collisional growth, radial drift, fragmentation, and vertical stirring by the Kelvin-Helmholtz instability. We show that satellitesimals can form in such CPDs if the dust-to-gas mass ratio of the inflow to the discs is larger than 0.02, which is 50 times smaller than the critical value in turbulent CPDs. This condition can be satisfied when enough amount of dust piles up at the gas pressure bump created by the planets. This result shows that satellitesimals would form in laminar CPDs with magnetic wind-driven accretion.

58. Velocity-Coherent Substructure in TMC-1: Inflow and Fragmentation

Simon E. T. Smith, Rachel Friesen, Antoine Marchal, Jaime E. Pineda, Paola Caselli, Michael Chun-Yuan Chen, Spandan Choudhury, James Di Francesco, Adam Ginsburg, Helen Kirk, Chris Matzner, Anna Punanova, Samantha Scibelli, Yancy Shirley ★ Filamentary structures have been found nearly ubiquitously in molecular clouds and yet their formation and evolution is still poorly understood. We examine a segment of Taurus Molecular Cloud 1 (TMC-1) that appears as a single, narrow filament in continuum emission from dust. We use the Regularized Optimization for Hyper-Spectral Analysis (ROHSA), a Gaussian decomposition algorithm which enforces spatial coherence when fitting multiple velocity components simultaneously over a data cube. We analyze HC_5N (9-8) line emission as part of the Green Bank Ammonia Survey (GAS) and identify three velocity-coherent components with ROHSA. The two brightest components extend the length of the filament, while the third component is fainter and clumpier. The brightest component has a prominent transverse velocity gradient of 2.7 ± 0.1 km s^{-1} pc^{-1} which we show to be indicative of gravitationally induced inflow. In the second component

we identify regularly spaced emission peaks along its length. We show that the local minima between pairs of adjacent HC_5N peaks line up closely with submillimetre continuum emission peaks, which we argue is evidence for fragmentation along the spine of TMC-1. While coherent velocity components have been described as separate physical structures in other star-forming filaments, we argue that the two bright components identified in HC_5N emission in TMC-1 are tracing two layers in one filament: a lower density outer layer whose material is flowing under gravity towards the higher density inner layer of the filament.

59. ALMA Fragmented Source Catalogue in Orion (FraSCO) I. Outflow interaction within an embedded cluster in OMC-2/FIR3, FIR4, and FIR5

Asako Sato, Satoko Takahashi, Shun Ishii, Paul T. P. Ho, Masahiro N. Machida, John Carpenter, Luis A. Zapata, Paula Stella Teixeira, Sümeyye Suri ★ We present a high angular resolution (~ 1") and wide-field ($2'.9 \times 1'.9$) image of the 1.3-mm continuum, CO($J = 2$–1) line, and SiO($J = 5$–4) line emissions toward an embedded protocluster, FIR3, FIR4, and FIR5, in the Orion Molecular Cloud 2 obtained from the Atacama Large Millimeter/submillimeter Array (ALMA). We identify 51 continuum sources, 36 of which are newly identified in this study. Their dust masses, projected sizes, and H_2 gas number densities are estimated to be 3.8×10^{-5}–$1.1 \times 10^{-2} M_\odot$, 290–2000 au, and 6.4×10^6–3.3×10^8 cm^{-3}, respectively. The results of a Jeans analysis show that ~ 80 % of the protostellar sources and ~ 15 % of the prestellar sources are gravitationally bound. We identify 12 molecular outflows traced in the CO($J = 2$–1) emission, six of which are newly detected. We spatially resolve shocked gas structures traced by the SiO($J = 5$–4) emission in this region for the first time. We identify shocked gas originating from outflows and other shocked regions. These results provide direct evidence of an interaction between a dust condensation, FIR4, and an energetic outflow driven by HOPS-370 located within FIR3. A comparison of the outflow dynamical timescales, fragmentation timescales, and protostellar ages shows that the previously proposed triggered star-formation scenario in FIR4 is not strongly supported. We also discuss the spatial distribution of filaments identified in our continuum image by comparing it with a previously identified hub-fiber system in the N_2H^+ line.

60. Three-dimensional Simulations of Magnetospheric Accretion in a T Tauri Star: Accretion and Wind Structures Just Around Star

Shinsuke Takasao, Kengo Tomida, Kazunari Iwasaki, Takeru K. Suzuki ★ We perform three-dimensional magneto-hydrodynamic simulations of magnetospheric accretion in a T Tauri star to study the accretion and wind structures in the close vicinity of the star. The gas accreting onto the star consists of the gas from the magnetospheric boundary and the failed disk winds. The accreting gas is commonly found as a multi-column accretion, which is consistent with observations. A significant fraction of the angular momentum of the accreting flows is removed by the magnetic fields of conical disk winds and turbulent failed winds inside and near the magnetosphere. As a result, the accretion torque is significantly reduced compared to the simple estimation based on the mass accretion rate. The stellar spin affects the time variability of the conical disk wind by changing the stability condition of the magnetospheric boundary. However, the time-averaged magnetospheric radius only weakly depends on the stellar spin, which is unlike the prediction of classical theories that the stellar spin controls the magnetospheric radius through the magnetic torque. The ratio of the toroidal to the poloidal field strengths at the magnetospheric boundary, which is a key parameter for the magnetic torque, is also insensitive to the spin; it is rather determined by the disk dynamics. Considering newly found three-dimensional effects, we obtain a scaling relation of the magnetospheric radius very similar to the Ghosh & Lamb relation from the steady angular momentum transport equation.

61. Planetesimal formation by the gravitational instability of dust ring structures

Sanemichi Z. Takahashi, Eiichiro Kokubo, Shu-ichiro Inutsuka ★ We investigate the gravitational instability (GI) of dust-ring structures and the formation of planetesimals by their gravitational collapse. The normalized dispersion relation of a self-gravitating ring structure includes two parameters that are related to its width and line mass (the mass per unit length). We survey these parameters and calculate the growth rate and wavenumber. Additionally, we investigate the planetesimal formation by growth of the GI of the ring that is formed by the growth of the secular GI of the protoplanetary disk. We adopt a massive, dust rich disk as a disk model. We find the range of radii for the fragmentation by the ring GI as a function of the width of the ring. The inner-most radius for the ring GI is smaller for the smaller ring width. We also determine the range of the initial planetesimal mass resulting from the fragmentation of the ring GI. Our results indicate that the planetesimal mass can be as large as 10^{28} g at its birth after the fragmentation. It can be as low as about 10^{25} g if the ring width is 0.1% of the ring radius and the lower limit increases with the ring width. Furthermore, we obtain approximate formulas for the upper and lower limits of the planetesimal mass. We predict that the planetesimals formed by the ring GI have prograde rotations because of the Coriolis force acting on the contracting dust. This is consistent with the fact that many trans-Neptunian binaries exhibit prograde rotation.

62. Hazy with a chance of star spots: constraining the atmosphere of the young planet, K2-33b

Pa Chia Thao, Andrew W. Mann, Peter Gao, Dylan A. Owens, Andrew Vanderburg, Elisabeth R. Newton, Yao Tang, Matthew J. Fields, Trevor J. David, Jonathan M. Irwin, Tim-Oliver Husser, David Charbonneau, Sarah Ballard ★ Although all-sky surveys have led to the discovery of dozens of young planets, little is known about their atmospheres. Here, we present multi-wavelength transit data for the super Neptune-sized exoplanet, K2-33b – the youngest (10 Myr) transiting exoplanet to-date. We combined photometric observations of K2-33 covering a total of 33 transits spanning >2 years, taken from K2, MEarth, Hubble, and Spitzer. The transit photometry spanned from the optical to the near-infrared (0.6-4.5μm), enabling us to construct a transmission spectrum of the planet. We find that the optical transit depths are nearly a factor of two deeper than those from the near-infrared. This difference holds across multiple datasets taken over years, ruling out issues of data analysis and unconstrained systematics. Surface inhomogeneities on the young star can reproduce some of the difference, but required spot coverage fractions (>60%) are ruled out by the observed stellar spectrum(<20%). We find a better fit to the transmission spectrum using photochemical hazes, which were predicted to be strong in young, moderate-temperature, and large-radius planets like K2-33b. A tholin haze with CO as the dominant gaseous carbon carrier in the atmosphere can reasonably reproduce the data with small or no stellar surface inhomogeneities, consistent with the stellar spectrum. The HST data quality is insufficient for the detection of any molecular features. More observations would be required to fully characterize the hazes and spot properties and confirm the presence of CO suggested by current data.

63. CARMA-NRO Orion Survey: unbiased survey of dense cores and core mass functions in Orion A

Hideaki Takemura, Fumitaka Nakamura, Héctor G. Arce, Nicola Schneider, Volker Ossenkopf-Okada, Shuo Kong, Shun Ishii, Kazuhito Dobashi, Tomomi Shimoikura, Patricio Sanhueza, Takashi Tsukagoshi, Paolo Padoan, Ralf S. Klessen, Paul. F. Goldsmith, Blakesley Burkhart, Dariusz C. Lis Álvaro Sánchez-Monge, Yoshito Shimajiri, Ryohei Kawabe ★ The mass distribution of dense cores is a potential key to understand the process of star formation. Applying dendrogram analysis to the CARMA-NRO Orion $C^{18}O$ (J=1–0) data, we identify 2342 dense cores, about 22 % of which have virial ratios smaller than 2, and can be classified as gravitationally bound cores. The derived core mass function (CMF) for bound starless cores which are not associate with protostars has a slope similar to Salpeter's initial mass function (IMF) for the mass range above 1 $M_\odot$, with a peak at $\sim$ 0.1 $M_\odot$. We divide the cloud into four parts based on the declination, OMC-1/2/3, OMC-4/5, L1641N/V380 Ori, and L1641C, and derive the CMFs in these regions. We find that starless cores with masses greater than 10 $M_\odot$ exist only in OMC-1/2/3, whereas the CMFs in OMC-4/5, L1641N, and L1641C are truncated at around 5–10 $M_\odot$. From the number ratio of bound starless cores and Class II objects in each subregion, the lifetime of bound starless cores is estimated to be 5–30 free-fall times, consistent with previous studies for other regions. In addition, we discuss core growth by mass accretion from the surrounding cloud material to explain the coincidence of peak masses between IMFs and CMFs. The mass accretion rate required for doubling the core mass within a core lifetime is larger than that of Bondi-Hoyle accretion by a factor of order 2. This implies that more dynamical accretion processes are required to grow cores.

64. Ionisation of inner T Tauri star discs: effects of in-situ energetic particles produced by strong magnetic reconnection events

Brunn V, Marcowith A, Sauty C, Padovani M, Rab C, Meskini C ★ Magnetic reconnection is one of the major particle acceleration processes in space and astrophysical plasmas. Low-energy supra-thermal particles emitted by magnetic reconnection are a source of ionisation for circumstellar discs, influencing their chemical, thermal and dynamical evolution. The aim of this work is to propose a first investigation to evaluate how energetic particles can propagate in the circumstellar disc of a T Tauri star and how they affect the ionisation rate of the disc plasma. To that end, we have collected experimental and theoretical cross sections for the production of H^+, H_2^+ and He^+ by electrons and protons. Starting from theoretical injection spectra of protons and electrons emitted during magnetic reconnection events, we have calculated the propagated spectra in the circumstellar disc considering the relevant energy loss processes. We have considered fluxes of energetic particles with different spectral indices and different disc magnetic configurations, generated at different positions from the star considering the physical properties of the flares as deduced from the observations obtained by the Chandra Orion Ultra Deep point source catalogue. We have then computed the ionisation rates for a disc whose structure has been calculated with the radiation thermo-chemical code `ProDiMo`. We find that energetic particles are potentially a very strong source of local ionisation with ionisation rates exceeding by several orders of magnitude the contribution due to X-rays, stellar energetic particles and radioactivity in the inner disc.

65. Formation of super-Earths in icy dead zones around low-mass stars

David Vallet, Anna C. Childs, Rebecca G. Martin, Mario Livio, Stephen Lepp ★ While giant planet occurrence rates increase with stellar mass, occurrence rates of close-in super-Earths decrease. This is in contradiction to the expectation that the total mass of the planets in a system scale with the protoplanetary disc mass and hence the stellar mass. Since the snow line

plays an important role in the planet formation process we examine differences in the temperature structure of protoplanetary gas discs around stars of different mass. Protoplanetary discs likely contain a dead zone at the midplane that is sufficiently cold and dense for the magneto-rotational instability to be suppressed. As material builds up, the outer parts of the dead zone may be heated by self-gravity. The temperature in the disc can be below the snow line temperature far from the star and in the inner parts of a dead zone. The inner icy region has a larger radial extent around smaller mass stars. The increased mass of solid icy material may allow for the in situ formation of larger and more numerous planets close to a low-mass star. Super-Earths that form in the inner icy region may have a composition that includes a significant fraction of volatiles.

66. A Census of Outflow to Magnetic Field Orientations in Nearby Molecular Clouds

Duo Xu, Stella S. R. Offner, Robert Gutermuth, Jonathan C. Tan ★ We define a sample of 200 protostellar outflows showing blue and redshifted CO emission in the nearby molecular clouds Ophiuchus, Taurus, Perseus and Orion to investigate the correlation between outflow orientations and local, but relatively large-scale, magnetic field directions traced by Planck 353 GHz dust polarization. At high significance (p 1e-4), we exclude a random distribution of relative orientations and find that there is a preference for alignment of projected plane of sky outflow axes with magnetic field directions. The distribution of relative position angles peaks at 30deg and exhibits a broad dispersion of 50deg. These results indicate that magnetic fields have dynamical influence in regulating the launching and/or propagation directions of outflows. However, the significant dispersion around perfect alignment orientation implies that there are large measurement uncertainties and/or a high degree of intrinsic variation caused by other physical processes, such as turbulence or strong stellar dynamical interactions. Outflow to magnetic field alignment is expected to lead to a correlation in the directions of nearby outflow pairs, depending on the degree of order of the field. Analyzing this effect we find limited correlation, except on relatively small scales < 0.5 pc. Furthermore, we train a convolutional neural network to infer the inclination angle of outflows with respect to the line of sight and apply it to our outflow sample to estimate their full 3D orientations. We find that the angles between outflow pairs in 3D space also show evidence of small-scale alignment.

67. Application of Convolutional Neural Networks to Predict Magnetic Fields Directions in Turbulent Clouds

Duo Xu, Chi-Yan Law, Jonathan C. Tan ★ We adopt the deep learning method CASI-3D (Convolutional Approach to Structure Identification-3D) to infer the orientation of magnetic fields in sub-/trans- Alfvenic turbulent clouds from molecular line emission. We carry out magnetohydrodynamic simulations with different magnetic field strengths and use these to generate synthetic observations. We apply the 3D radiation transfer code RADMC-3d to model 12CO and 13CO (J = 1-0) line emission from the simulated clouds and then train a CASI-3D model on these line emission data cubes to predict magnetic field morphology at the pixel level. The trained CASI-3D model is able to infer magnetic field directions with low error ($<$ 10deg for sub-Alfvenic samples and $<$30deg for trans-Alfvenic samples). We furthermore test the performance of CASI-3D on a real sub-/trans- Alfvenic region in Taurus. The CASI-3D prediction is consistent with the magnetic field direction inferred from Planck dust polarization measurements. We use our developed methods to produce a new magnetic field map of Taurus that has a three-times higher angular resolution than the Planck map.

68. CORINOS I: JWST/MIRI Spectroscopy and Imaging of a Class 0 protostar IRAS 15398-3359

Yao-Lun Yang, Joel D. Green, Klaus M. Pontoppidan, Jennifer B. Bergner, L. Ilsedore Cleeves, Neal J. Evans II, Robin T. Garrod, Mihwa Jin, Chul Hwan Kim, Jaeyeong Kim, Jeong-Eun Lee, Nami Sakai, Christopher N. Shingledecker, Brielle Shope, John J. Tobin, Ewine van Dishoeck ★ The origin of complex organic molecules (COMs) in young Class 0 protostars has been one of the major questions in astrochemistry and star formation. While COMs are thought to form on icy dust grains via gas-grain chemistry, observational constraints on their formation pathways have been limited to gas-phase detection. Sensitive mid-infrared spectroscopy with JWST enables unprecedented investigation of COM formation by measuring their ice absorption features. We present an overview of JWST/MIRI MRS spectroscopy and imaging of a young Class 0 protostar, IRAS 15398-3359, and identify several major solid-state absorption features in the 4.9-28 μm wavelength range. These can be attributed to common ice species, such as H_2O, CH_3OH, NH_3, and CH_4, and may have contributions from more complex organic species, such as C_2H_5OH and CH_3CHO. The MRS spectra show many weaker emission lines at 6-8 μm, which are due to warm CO gas and water vapor, possibly from a young embedded disk previously unseen. Finally, we detect emission lines from [Fe II], [Ne II], [S I], and H_2, tracing a bipolar jet and outflow cavities. MIRI imaging serendipitously covers the south-western (blue-shifted) outflow lobe of IRAS 15398-3359, showing four shell-like structures similar to the outflows traced by molecular emission at sub-mm wavelengths. This overview analysis highlights the vast potential of JWST/MIRI observations and previews scientific discoveries in the coming years.

69. Increasing mass-to-flux ratio from the dense core to the protostellar envelope around the Class 0 protostar HH 211

Hsi-Wei Yen, Patrick Koch, Chin-Fei Lee, Naomi Hirano, Nagayoshi Ohashi, Jinshi Sai, Shigehisa Takakuwa, Ya-Wen Tang, Ken'ichi Tatematsu, Bo Zhao ★ To study transportation of magnetic flux from large to small scales in protostellar sources, we analyzed the Nobeyama 45-m N2H+ (1-0), JCMT 850 um polarization, and ALMA C18O (2-1) and 1.3 mm and 0.8 mm (polarized) continuum data of the Class 0 protostar HH 211. The magnetic field strength in the dense core on a 0.1 pc scale was estimated with the single-dish line and polarization data using the Davis-Chandrasekhar-Fermi method, and that in the protostellar envelope on a 600 au scale was estimated from the force balance between the gravity and magnetic field tension by analyzing the gas kinematics and magnetic field structures with the ALMA data. Our analysis suggests that from 0.1 pc to 600 au scales, the magnetic field strength increases from 40-107 uG to 0.3-1.2 mG with a scaling relation between the magnetic field strength and density of $B \propto \rho^{0.36\pm0.08}$, and the mass-to-flux ratio increases from 1.2-3.7 to 9.1-32.3. The increase in the mass-to-flux ratio could suggest that the magnetic field is partially decoupled from the neutral matter between 0.1 pc and 600 au scales, and hint at efficient ambipolar diffusion in the infalling protostellar envelope in HH 211, which is the dominant non-ideal magnetohydrodynamic effect considering the density on these scales. Thus, our results could support the scenario of efficient ambipolar diffusion enabling the formation of the 20 au Keplerian disk in HH 211.

70. OH mid-infrared emission as a diagnostic of H_2O UV photodissociation. II. Application to interstellar PDRs

Marion Zannese, Benoît Tabone, Emilie Habart, Franck Le Petit, Ewine F. van Dishoeck, Emeric Bron ★ Water photodissociation in the 114 - 144 nm UV range forms excited OH which emits at mid-infrared wavelengths via highly excited rotational lines. These lines have only been detected with Spitzer in several proto-planetary disks and shocks. Previous studies have shown they are a unique diagnostic for water photodissociation. Thanks to its high sensitivity and angular resolution, the James Webb Space Telescope (JWST) could be able to detect them in other environments such as interstellar Photo-Dissociation Regions (PDRs). In order to predict the emerging spectrum of OH, we use the Meudon PDR Code to compute the thermal and chemical structure of PDRs. The influence of thermal pressure ($P_{\rm th}/k = n_{\rm H}T_{\rm K}$) and UV field strength on the integrated intensities, as well as their detectability with the JWST are studied in details. OH mid-IR emission is predicted to originate very close to the H^0/H_2 transition and is directly proportional to the column density of water photodissociated in that layer. Because neutral gas-phase formation of water requires relatively high temperatures ($T_{\rm K} \gtrsim 300$ K), the resulting OH mid-IR lines are primarily correlated with the temperature at this position, and are therefore brighter in regions with high pressure. This implies that these lines are predicted to be only detectable in strongly irradiated PDRs ($G_0^{\rm incident} > 10^3$) with high thermal pressure ($P_{\rm th}/k \gtrsim 5{\times}10^7$ K cm^{-3}). In the latter case, OH mid-IR lines are less dependent on the strength of the incident UV field. The detection in PDRs like the Orion bar, which should be possible, is also investigated. To conclude, OH mid-IR lines observable by JWST are a promising diagnostics for dense and strongly irradiated PDRs.

71. Radial Velocity Survey for Planets around Young stars (RVSPY) A transiting warm super-Jovian planet around HD 114082, a young star with a debris disk

O. Zakhozhay, R. Launhardt, T. Trifonov, M. Kürster, S. Reffert, Th. Henning, R. Brahm, J. Vinés, G. -D. Marleau, J. Patel ★ Aiming to detect planetary companions to young stars with debris disks via the radial velocity method, we observed HD114082 during April 2018 - August 2022 as one of the targets of our RVSPY program (Radial Velocity Survey for Planets around Young stars). We used the FEROS spectrograph, mounted to the MPG/ESO 2.2 m telescope in Chile, to obtain high signal-to-noise spectra and time series of precise radial velocities (RVs). Additionally, we analyzed archival HARPS spectra and TESS photometric data. We used the CERES, CERES++ and SERVAL pipelines to derive RVs and activity indicators and ExoStriker for the independent and combined analysis of the RVs and TESS photometry. We report the discovery of a warm super-Jovian companion around HD114082 based on a 109.8±0.4 day signal in the combined RV data from FEROS and HARPS, and on one transit event in the TESS photometry. The best-fit model indicates a 8.0±1.0 Mjup companion with a radius of 1.00±0.03 Rjup in an orbit with a semi-major axis of 0.51±0.01 au and an eccentricity of 0.4±0.04. The companions orbit is in agreement with the known near edge-on debris disk located at about 28 au. HD114082b is possibly the youngest (15±6 Myr), and one of only three younger than 100 Myr giant planetary companions for which both their mass and radius have been determined observationally. It is probably the first properly model-constraining giant planet that allows distinguishing between hot and cold-start models. It is significantly more compatible with the cold-start model.

72. WISE Green Objects (WGOs): the massive star candidates in the whole Galactic Plane ($|\ b\ | < 2^\circ$)

Chang Zhang, Guo-Yin Zhang, Jin-Zeng Li, Jing-Hua Yuan ★ Massive young stellar objects (MYSOs) play a crucial role in star formation. Given that MYSOs were previously identified based on the extended structure and the observational data for them is limited, screening the Wide-field Infrared Survey Explorer (WISE) objects showing green features (for the common

coding of the 4.6 μm band as green channel in three-color composite WISE images) will yield more MYSO candidates. Using WISE images in the whole Galactic Plane ($0^\circ < l < 360^\circ$ and $\mid b \mid < 2^\circ$), we identified sources with strong emissions at 4.6 μm band, then according to morphological features divided them into three groups. We present a catalog of 2135 WISE Green Objects (WGOs). 264 WGOs have an extended structure. 1366 WGOs show compact green feature but without extended structure. 505 WGOs have neither extended structure nor green feature, but the intensity at 4.6 μm is numerically at least 4.5 times that of 3.4 μm. According to the analysis of the coordinates of WGOs, we find WGOs are mainly distributed in $\mid l \mid < 60^\circ$, coincident with the position of the giant molecular clouds in $\mid l \mid > 60^\circ$. Matching results with various masers show that those three groups of WGOs are at different evolutionary stages. After cross-matching WGOs with published YSO survey catalogs, we infer that $\sim$50% of WGOs are samples of newly discovered YSOs. In addition, 1260 WGOs are associated with Hi-GAL sources, according to physical parameters estimated by spectral energy distribution fitting, of which 231 are classified as robust MYSOs and 172 as candidate MYSOs.